This is to certify that the

dissertation entitled

A Two Part Study: Morphology, Cytology and Synaptic Relations of Primary Trigeminal Axons Terminating in the Dorsomedial Subdivision of Rat Trigeminal Nucleus Oralis and Comparison of the Distribution and Morphology of Neurons in Rat Trigeminal Nucleus Oralis Projecting to Facial, Hypoglossal and Trigeminal Motor Nuclei.

presented by

Deborah J. Sohn

has been accepted towards fulfillment
of the requirements for

Ph.D. degree in Anatomy

William Mdalls PhD
Major professor

Date 11-17-94

A TWO PART STUDY:

MORPHOLOGY, CYTOLOGY AND SYNAPTIC RELATIONS OF PRIMARY TRIGEMINAL AXONS TERMINATING IN THE DORSOMEDIAL SUBDIVISION OF RAT TRIGEMINAL NUCLEUS ORALIS AND COMPARISON OF THE DISTRIBUTION AND MORPHOLOGY OF NEURONS IN RAT TRIGEMINAL NUCLEUS ORALIS PROJECTING TO FACIAL, HYPOGLOSSAL AND TRIGEMINAL MOTOR NUCLEI

By

Deborah J. Sohn

A DISSERTATION

Submitted to
Michigan State University
in partial fulfillment of the requirements
for the degree of

DOCTOR OF PHILOSOPHY

Department of Anatomy

1994

ABSTRACT

MORPHOLOGY, CYTOLOGY AND SYNAPTIC RELATIONS OF PRIMARY TRIGEMINAL AXONS TERMINATING IN THE DORSOMEDIAL SUBDIVISION OF RAT TRIGEMINAL NUCLEUS ORALIS
AND
COMPARISON OF THE DISTRIBUTION AND MORPHOLOGY OF NEURONS IN RAT TRIGEMINAL NUCLEUS ORALIS PROJECTING TO FACIAL, HYPOGLOSSAL AND TRIGEMINAL MOTOR NUCLEI

By

Deborah J. Sohn

Two studies were completed in rat trigeminal nucleus oralis (Vo). In the first, anterograde transport of horseradish peroxidase (HRP) was used to examine the overall morphology, distribution, cytology and synaptic relations of primary trigeminal axons terminating in the dorsomedial (DM) subdivision of Vo. Injections into the sensory root of the trigeminal nerve labeled axons throughout DM. Light microscopic analyses revealed that DM receives terminal arborizations of two morphologically distinct types (Type I and Type II) of primary axons. Type I primary axons were a direct continuation of parent fibers travelling dorsomedially in the spinal trigeminal tract (SVT) and terminating as a sparsely branched, long, medially directed terminal strand containing up to thirty-three boutons. Type II primary axons arose as medially directed collaterals from parent branches ascending dorsomedially in SVT. Within DM they divided into two to four medially directed terminal strands containing one to nineteen boutons. Electron microscopic analyses reveal that primary axonal endings from

Type I afferents are found singly or in a simple glomerulus while Type II primary endings are found in complex glomerular arrangements. Type I and Type II primary endings contain agranular spherical synaptic vesicles and make axodendritic synapses on dendritic shafts. This suggests that at least two types of orofacial sensory inputs are being conveyed to DM neurons. In the second study retrograde horseradish peroxidase (HRP) transport was used to examine and compare the overall distribution and morphology of neurons in Vo projecting to facial (VII), hypoglossal (XII) and trigeminal (Vmo) motor nuclei. Injections into VII and Vmo labeled different types of neurons in ventrolateral (VL) and DM subdivisions throughout the middle third of Vo. Injections in XII labeled nearly equal numbers of VL and DM neurons in the middle third of Vo. These results suggest that there are morphologically distinct populations of neurons in the middle third of VL and DM projecting to VII, Vmo and XII. Vo involvement in complex orofacial reflexes is suggested by these findings.

DEDICATION

To my sons, Richard and Derek

ACKNOWLEDGEMENT

I would like to express my deepest gratitude and sincere appreciation to my advisor, Dr. William McKenzie Falls, for his unwavering patience, support, encouragement and guidance throughout my graduate studies. I also wish to thank the members of my graduate committee: Drs. Robert Bowker, Irena Grofova, John Johnson, Frank Pansino, and Charles Tweedle for their support and guidance.

I would like to extend my gratitude to the faculty and staff of the Department of Anatomy well as my fellow graduate students for their friendship, encouragement and technical assistance.

Although many individuals are remembered for their generosity and support, my greatest strength comes from my loving family and friends whose unconditional love helped me to achieve my goals.

TABLE OF CONTENTS

LIST OF FIGURES

CHAPTER I

Chapter II

ABBREVIATIONS

BZ	border zone Vo
CDM	caudal dorsomedial subdivision
DAB	3,3′ diaminobenzidine tetrachloride
DM	dorsomedial Vo
DMSO	dimethysulfoxide
F	flattened synaptic vesicles
HRP	horseradish peroxidase
IS	injection site
MDH	trigeminal nucleus caudalis (medullary dorsal horn)
MDM	middle dorsomedial subdivision
MDMd	middle dorsal zone of DM
MDMv	middle ventral zone of DM
P	pleomorphic synaptic vesicles
PHA-L	phaseolus vulgaris leucoagglutinin
P1	primary axonal ending type I
P2	primary axonal ending type II
R	large round synaptic vesicles
r	small round synaptic vesicles
RDM	rostral dorsomedial subdivision
SVN	spinal trigeminal nucleus
SVT	spinal trigeminal tract

TSNC	trigeminal sensory nuclear complex
Vi	trigeminal nucleus interpolaris
VII	facial motor nucleus
VL	ventrolateral Vo
Vmo	trigeminal motor nucleus
Vms	main sensory trigeminal nucleus
Vo	trigeminal nucleus oralis
XII	hypoglossal nucleus

INTRODUCTION

Trigeminal nucleus oralis (Vo), the most rostral subdivision of the mammalian spinal trigeminal nucleus (SVN),is thought to play a significant role in the reception, central processing, modification and the transmission of nociceptive information to the brainstem and spinal cord from tooth pulp, oral and perioral areas as well as mechanoreceptive information from the face and oral cavity. Ithas been determined through anatomical and electrophysiological techniques in a variety of mammals that axons of primary trigeminal neurons terminate in Vo (1,3,10,19,20,23). Rat Vo can be divided into three subdivisions on the basis of several morphological and functional criteria: ventrolateral (VL), border zone (BZ), and dorsomedial (DM) (14,15,16,17,18, 19,23,24,26,34,36).

Numerous anatomical, electrophysiological and electron microscopic studies have been completed in order to discern the anatomic and functional organization of Vo (1,6,8,9,15,16, 17,18,19,20,21,22,23,24,25,29,33,36,53,58,60,64,65,68). However, this information is still incomplete in regards to DM. The first part of the present study uses light microscopy to evaluate the overall morphology of primary

trigeminal afferent axons terminating in DM and electron microscopy to evaluate their cytology and synaptic relations. Comparisons are made with primary trigeminal afferent axons terminating in BZ and VL. The second part of this study uses retrograde transport of horseradish peroxidase at the light microscopic level to study the morphology and distribution of Vo neurons projecting to facial (VII), hypoglossal (XII) and trigeminal (Vmo) motor nuclei. Taken together these studies add further insight into understanding the anatomical framework and circuitry through which Vo receives, processes and transmits orofacial mechanoreceptive and nociceptive information.

CHAPTER I

MORPHOLOGY, CYTOLOGY AND SYNAPTIC RELATIONS OF PRIMARY TRIGEMINAL AXONS TERMINATING IN THE DORSOMEDIAL SUBDIVISION OF RAT TRIGEMINAL NUCLEUS ORALIS

INTRODUCTION

Knowledge of the normal central processing of nociceptive information from the orofacial region is necessary in order to help devise methods to decrease and/or eliminate acute and chronic pain syndromes which accompany craniomandibular/ craniovertebral dysfunction. Neuroanatomical studies and electrophysiological investigations have shown that the spinal trigeminal nucleus (SVN) and the main sensory trigeminal nucleus (Vms) receive, process, modify, and relay primary afferent somatosensory information from the teeth, facial skin, oral and nasal cavities, temporomandibular joint and the cornea(2,4,5,6,7,9,16,17,41,43,45,48,49,50,51,54,58,61,62,66). The mammalian SVN can be divided into three cytoarchitecturally distinct nuclei: a rostrally situated trigeminal nucleus oralis (Vo), an intermediate trigeminal nucleus interpolaris (Vi) and a caudally located trigeminal nucleus caudalis, also referred to as the medullary dorsal horn (MDH) to reflect its structural and functional

similarities to the spinal dorsal horn (32,38,61).

Utilizing anatomical and electrophysiological techniques in a variety of mammals, central axons of primary trigeminal neurons have been shown to terminate in Vo (1,3,10,19,20,23, 4,36,43,44,54,60,61,62,68,69). Rat Vo receives nociceptive as well as mechanoreceptive primary afferent information and is involved in the central processing, modification, and transmission of this information from oral and perioral areas, face and oral cavity, temporomandibular joint and tooth pulp (3,4,5,9,16,34,36,50,58,60,61,62,66,69). Nociceptive input from the tooth pulp, oral and perioral areas is thought to reach second-order Vo neurons by way of small myelinated Aσ and unmyelinated C primary trigeminal axons while mechanoreceptive information from the face and peripheral receptive fields located in the oral cavity are thought to be conveyed to second-order Vo neurons by way of Aσ and larger myelinated Aβ primary axons (14,15,16,17,18,19,20,23,24,25, 26,34,35).

On the basis of several morphological and functional criteria, rat Vo can be divided into ventrolateral (VL), dorsomedial (DM), and border zone (BZ) subdivisions, (16,17, 18). By correlating the Golgi method with retrograde horseradish peroxidase (HRP) labeling, VL has been shown to contain three morphologically distinct types of neurons which project to MDH in the rat (18) and cat (37). Retrograde HRP labeling studies in the rat have identified VL trigeminospinal

projection neurons, innervating all spinal cord levels (17,47, 57) and Golgi studies have identified a VL Golgi type II interneuron (14). Trigeminofacial projection neurons (12,13), trigeminothalamic neurons, (8,13,27,63) and trigeminotectal projection neurons (8,39) have also been shown to be present in VL. Anterograde studies utilizing phaseolus vulgaris leucoagglutinin (PHA-L) have shown that injections into rat VL result in labeled terminal axonal arbors in the cervical and thoracic spinal cord, cerebellum, thalamus, solitary nucleus, ipsilateral and contralateral SVN, as well as Vmo, VII and XII motor nuclei (64). In addition, two groups of ascending intratrigeminal axons originating from MDH neurons (16) and a population of small myelinated primary trigeminal axons arborize within VL (20,22) and are in a position to provide input directly to VL neurons.

Using anterograde transport of HRP, BZ has been found to receive the terminal arborizations of five distinct populations of primary trigeminal axons. One population is derived from small myelinated parent axons and is found throughout BZ (21,22,23,24) while a second population originates from unmyelinated parent axons which terminate in the dorsal one-half of the subdivision (22,23). The three remaining populations arise from different types of large myelinated fibers (21). Additional studies have revealed that after PHA-L injections into BZ, anterograde labeling of terminal axonal arbors can be found in cervical and thoracic

spinal cord, cerebellum, thalamus, VII, Vmo, solitary nucleus and SVN (64). BZ also contains the terminal axonal arbors of one group of ascending intratrigeminal axons from MDH neurons (16). Retrograde HRP studies have shown a variety of projection neurons to be present in the subdivision. A single population of trigeminocerebellar projection neurons is situated in the dorsal portion of BZ (23) while descending MDH projection neurons (16) are located in the ventral portions of BZ. Small populations of morphologically distinct trigeminotectal (8), trigeminospinal (17), and trigeminothalamic (8) projection neurons are also found throughout the subdivision.

To date, electron microscopic analyses provide evidence that at least three distinct types of synaptic glomeruli exist in VL and BZ (22). Each glomerulus contains a primary trigeminal afferent axonal ending. It is within these glomeruli that the fundamental principles of structural and functional organization of VL and BZ are found. Within BZ, two types of glomeruli have been identified: one containing the axonal ending of a small myelinated primary trigeminal axon and the other which includes the terminal of an unmyelinated primary axon. The primary ending terminating in BZ, derived from small myelinated parent fibers, lies centrally in the glomerulus making at least one axodendritic synapse with one to two dendritic shafts, while the ending of the unmyelinated primary axon lies at the periphery of the

glomerulus where it forms a single axodendritic synapse on a central dendrite. Axonal endings of small myelinated primary trigeminal axons were found to lie centrally in identified glomeruli in VL and they formed axodendritic synapses on numerous dendritic shafts and spines. It is believed that the transfer of information from these three populations of primary axons directly to the dendritic arbors of second-order BZ and VL neurons occurs at the asymmetrical axodendritic synapses. All of the above studies continue to provide evidence that each Vo subdivision, especially VL and BZ, is morphologically and functionally distinct. However, further analyses, similar to those presented above, are needed with regard to DM in order to substantiate the view that all of Vo is an important part of SVN involved in the reception, central processing and modification and relay of nociceptive and mechanoreceptive information and that each subdivision is morphologically and functionally distinct. To date, retrograde studies have shown that within DM there are five morphologically distinct types of trigeminocerebellar projection neurons, all of which innervate one or more of the orofacial portions of four major tactile areas in the rat cerebellar cortex (26). Furthermore, injections of PHA-L into DM have labeled terminal axonal arbors at all levels of the rat spinal cord, cerebellum, thalamus, solitary nucleus, SVN bilaterally as well as Vmo, VII and XII (64).

In this anterograde HRP study, light microscopic techniques were utilized to evaluate the overall morphology of primary trigeminal afferent axons terminating in DM. In addition, electron microscopy was used to examine the labeled axons and synaptic relations of their terminal endings. Comparisons between these data and data on the primary trigeminal axons already identified in VL and BZ is discussed to help distinguish each subdivision's relationship to one another as well as to SVN as a whole.

MATERIALS AND METHODS

Five adult male Sprague-Dawley albino rats (250-300 grams) were anesthetized with sodium pentobarbital (35-40mg/kg) and positioned in a stereotaxic apparatus (Kopf Instruments). All surgical procedures were performed using aseptic technique. The cranium was opened unilaterally in the parietal bone, the dural sheath incised and the cerebral cortex overlying the sensory root and ganglion of the trigeminal nerve was removed by suction. Dense connective tissue and bone covering the sensory root of the trigeminal nerve was removed to allow full exposure. Approximately 10μl of 30% HRP (Sigma Type VI) in 2% dimethylsulfoxide (DMSO) was injected manually into the sensory root of each animal. Under visual guidance, multiple injections (0.05-1.0μl HRP per injection) were delivered over a 5-minute period using a 31-gauge needle connected to a 10μl Hamilton Syringe. Following termination of the injections, the needle was left in place in the sensory root for an additional 5 minutes and then withdrawn. Upon completion of the experiment, gelfoam (UpJohn Company) was positioned in the opening, the incision was clamped closed and an application of triple antibiotic ointment (Rugby Laboratories) was placed over the incision site. All animals were housed, maintained and cared for according to federally prescribed guidelines (52). After postinjection survival periods of 48-72 hours, the animals

were deeply anesthetized and perfused transcardially with a fixative solution (1000 ml) containing 2% paraformaldehyde and 2% glutaraldehyde in a 0.15M phosphate buffer (pH 7.3). The brain was removed immediately and postfixed overnight at 4°C. The following day the brainstem, along with the sensory root containing the trigeminal sensory nuclear complex (TSNC), was cut on an Oxford Vibratome into 100μm thick serial sections in either the transverse or horizontal planes and collected in tissue trays containing 0.15M phosphate buffer. All sections were processed immediately using the cobalt-glucose oxidase technique (42). Sections were rinsed twice in 0.1M Tris buffer for 5 minutes each, followed by cobalt chloride pretreatment (filtered 0.5% $CoCl_2$ solution in 0.1M Tris buffer) for 10 minutes. After washing the sections (3 minutes) in Tris buffer, they were laced in fresh 0.15M phosphate buffer. A solution composed of 200 ml of 0.15% phosphate buffer and 0.1g 3,3′ diaminobenzidine tetrachloride or DAB (Sigma) was mixed and filtered; 0.4g B-D(+) glucose, 0.08g ammonium chloride, and 0.0006g glucose oxidase were added to the solution. Sections were incubated in this solution for 30 minutes, then rinsed with 0.15M phosphate buffer. These steps were repeated for a total of three incubations of DAB. After rinsing the sections twice in 0.15M phosphate buffer, they were cleared through a graded series of glycerin concentrations (20%, 40%, 60%, 80%, 100%), placed on glass slides in 100% glycerin and coverslipped for light

microscopic analysis. All sections were analyzed in order to ascertain the overall morphology of labeled primary trigeminal axons and where they were terminating in the TSNC as well as their trajectory through the spinal trigeminal tract (SVT), the root entry zone and the sensory root proximal to the injection site. Some sections demonstrating completely labeled primary trigeminal axons in DM of Vo were processed for electron microscopic analysis according to the procedure of Gobel et al. (32). The remaining sections were rehydrated through a descending series of glycerin concentrations, (100%. 80%, 60%, 40%, 20%), rinsed in a 0.15M phosphate buffer, mounted on gelatin-coated glass slides, counterstained with cresyl violet and coverslipped. These sections were extensively evaluated to determine the overall course, distribution, organization and morphology of labeled primary trigeminal axons at the light microscopic level using a Leitz Laborlux 12 microscope fitted with a drawing tube. Detailed drawings of HRP-labeled primary trigeminal axons were made under a 100X oil immersion objective lens at a magnification of 1,250X to demonstrate parent branches in SVT, as well as collaterals and terminal arborizations in DM. Photomicrographs of corresponding sections were taken to illustrate morphological details. Those sections containing completely labeled primary trigeminal axons in DM were trimmed and processed for electron microscopy. These sections were transferred back through a descending series of glycerin

concentrations, rinsed in 0.15M phosphate buffer, and post-fixed in 2% osmium tetroxide containing 8.5% dextrose in 0.15M phosphate buffer for one hour at room temperature. After rinsing in distilled water, the sections were block stained with 1% uranyl acetate (in distilled water) for 24 hours at room temperature. Sections were dehydrated for 60 minutes through a graded series of ethanol concentrations (50%, 70%, 80%, 90%, 100%) followed by 50 minutes of soaking in propylene oxide (three changes for 10 minutes, 10 minutes, and 30 minutes). After the sections were soaked in a 1:1 ratio of propylene oxide and Marglas for 30-45 minutes, they were infiltrated with 100% Marglas for 24 hours. Shallow molds were used to flat embed the sections in fresh Marglas and they were polymerized at 60°C for 24 hours. The blocks were mounted in specimen holders of a Sorvall MT-2 ultramicrotome and trimmed to the area containing the labeled primary axons in DM which were previously drawn. One or two μm thick sections were cut to further identify and localize the fibers. The blocks were then serially thin-sectioned with the sections mounted on Formvar coated slotted grids and viewed with a transmission electron microscope (CM10). Electron micrographs were made from serial thin-sections and examined. The cytology and synaptic relationships of the labeled primary axons were evaluated. Each axon, its terminal arbors and endings were analyzed with regard to size, shape and relationship to other axons, dendrites, and cell bodies as well as synaptic

junctional morphology. Cytoplasmic contents were identified and presynaptic and postsynaptic structures, including site of termination, were classified.

RESULTS

LIGHT MICROSCOPY

Following the injections, many primary trigeminal axons located in SVT, the root entry zone and the sensory root of the trigeminal nerve are filled with HRP reaction product. These regions contralaterally contain no labeled fibers. Throughout Vo primary trigeminal axons form terminal arborizations in each of the three nuclear subdivisions, VL, BZ, and DM. Within DM, primary trigeminal afferent terminal arborizations are found in each of its four portions: rostral (RDM), middle ventral zone (MDMv), middle dorsal zone (MDMd), and caudal (CDM). On the basis of their overall morphology and manner of termination, primary trigeminal axons terminating in each portion of DM can be classified into two specific types (Type I and Type II).

The Type I primary trigeminal afferent axon (Figure 1) is a direct continuation of its parent fiber traveling caudally in the dorsomedial portion of SVT. Upon entering Vo, the axon does not branch as it traverses BZ and terminates in DM as a long medially directed unbranched terminal strand, 425-650μm in length (Figure 1). Measurements of the diameter of eighteen parent fibers and terminal strands show that along their course, these axons vary in thickness from 1-2.5 μm at their maximum diameter (Figures 1, 4). They could never be traced back to thicker primary axons in either SVT or the

sensory root. Along each terminal strand are fourteen to thirty-three irregularly spaced boutons with one bouton always found at the terminal end of each strand (Figures 1, 4). Boutons along any one terminal strand may vary in size and shape, ranging from 1-4μm at their maximum diameter and displaying spherical to elliptical shapes. Type I primary trigeminal axons appear to terminate in equal density throughout all four portions of DM.

Parent fibers of the Type II primary trigeminal axon are also confined to and descend in dorsomedial SVT. Unlike Type I parent fibers,these parent axons travel through the root entry zone and within SVT give rise to medially directed collaterals as they descend in SVT. The collaterals traverse BZ and enter DM (Figure 2). Measurements of the parent axons in the root entry zone and in SVT, as well as the collaterals in SVT and DM show that they range in thickness from 2-4μm and 3-5μm, respectively, at their maximum diameter. Upon entering DM, the collaterals divide into two to four medially directed terminal strands (Figures 2,3). Each strand extends from 28-74 μm in length. The resulting cone-shaped dendritic arbors (with the apex at or near to BZ-DM border) spread out mediolaterally, rostrocaudally and dorsoventrally for 17-93 μm. Located along each of the collaterals and their terminal strands are one to nineteen irregularly spaced boutons, with one always located at the terminal tip of each strand (Figures 2,3). The boutons vary in shape from spherical to elliptical

and measure 1-6μm along their maximum diameter. Type II terminal arborizations are confined to DM and are found in all four portions of the subdivision, with the majority found in MDMv.

ELECTRON MICROSCOPY

Electron microscopic analyses of isolated HRP-labeled parent branches and collaterals of Type I and Type II primary trigeminal axons, terminating in DM reveal that they are thinly myelinated (Figure 5). The myelin sheaths of Type I parent axons measure 0.01 to 0.10 μm in thickness while those of Type II parent axons and collaterals range from 0.1 to 1.5 μm in thickness (Figure 5). The terminal strands of both populations of primary trigeminal axons are unmyelinated (Figure 8). These findings substantiate the light microscopical findings for the diameters of other Type I and Type II HRP-filled parent fibers and for the Type II collaterals entering DM as well as for the terminal strands from both populations of primary trigeminal axons arborizing in DM.

Throughout the DM neuropil, primary (PR) axonal endings from Type I afferents are found singly or on occasion in a simple glomerulus (Figures 6,8,9,10) while all of those from Type II afferents are found in a complex glomerular arrangement (Figures 7,11,12, 13). The PR endings of each afferent type are morphologically different and can be distinguished from each other on the basis of their cytology

and synaptic relations (Figures 6,7).

Type I Primary Endings(P1): The P1 endings present either an elongated scalloped appearance (Figures 6,8) or a simple dome shape (Figures 9,10). They are filled with a single population of agranular spherical (45-60 nm in diameter) synaptic vesicles which are closely packed and fill the entire ending (Figures 6,8,9,10). P1 endings form asymmetrical synaptic junctions with dendritic shafts. These axodendritic synaptic junctions may be either single or multiple on the same dendritic shaft (Figures 6,8,9,10). A P1 ending synapses on a single dendritic shaft and does not make synaptic contact with multiple dendrites or dendritic spines. These dendritic shafts exhibit the cytoplasmic characteristics of distal dendritic branches, i.e. they are 1.5 μm or less in diameter and contain neurofilaments, microtubules, agranular endoplasmic reticulum and mitochondria. Most Type I endings are completely surrounded by overlapping astrocytic processes except at the synaptic junction. Unlabeled axonal endings are also found around the postsynaptic dendritic shaft (Figure 6,9). The most common is a small dome shaped ending containing small round synaptic vesicles (r ending; 35-40nm in diameter). This ending makes an asymmetrical axodendritic synapse with the postsynaptic dendritic shaft.

On occasion a Type I ending will be found in a simple glomerulus (Figures 6,10). Here the Type I ending is not only presynaptic to a dendritic shaft but is also postsynaptic to

a single unlabeled axonal ending (P ending). This P ending containing scattered pleomorphic synaptic vesicles (40-50nm in diameter) makes an axoaxonic synaptic contact which is characterized by a single symmetrical to intermediate type synaptic junction. The P ending does not synapse on the dendritic shaft which is postsynaptic to the PR ending. The PR and P endings are surrounded by astrocytic processes.

Type II PR Endings(P2): The P2 endings present a scalloped to dome-shaped outline and each lies at the periphery of a glomerulus containing a central dendrite, unmyelinated axons and three different types of unlabeled axonal endings each with different populations of synaptic vesicles (Figures 7,11,12,13). All of these neuronal elements are surrounded by overlapping thick and sheet-like astrocytic processes. Type II Primary endings contain agranular spherical (45 to 60 nm in diameter) synaptic vesicles among which are scattered several spherical dense core vesicles (85 to 100 nm in diameter; Figures 7,11). The synaptic vesicles are dispersed throughout the terminal cytoplasm and are aggregated at the asymmetrical synaptic junctions associated with each P2 ending (Figures 12, 13c).In each glomerulus, a Type II Primary ending makes synaptic contact with the central dendritic shaft (Figures 7,12,13c). This dendritic shaft possesses the cytoplasmic characteristics typical of distal dendritic branches and receives at least one and often multiple asymmetrical axodendritic synapses from the P2 ending

(Figures 7,12,13c). In addition, a single dendritic shaft receives synapses from multiple P2 endings originating from the same axon, but each involved in separate glomeruli. In this study there were no instances where dendritic shafts were found to contain agranular synaptic vesicles, nor were they observed to participate in either dendrodendritic or dendroaxonic synapse. Furthermore, PR endings were never observed to be in contact with dendritic spines.

Small neuronal processes containing synaptic vesicles are commonly found in the glomeruli containing P2 endings (Figures 7,12,13). They are considered to be axonal endings because they arise from many of the unmyelinated axons coursing through the glomeruli and because they, as well as their unmyelinated parent branches, have never been observed to be postsynaptic to the P2 endings. These axonal endings can be divided into three distinct types on the basis of the size and shape of their synaptic vesicles and the morphological type of synaptic junction they establish with their postsynaptic neuronal elements.The most prevalent small axonal ending is called the F ending because it contains predominantly flattened agranular synaptic vesicles measuring 60X30 nm across their long and short axes, respectively (Figures 7,13). On the average, two F endings are found in any one glomerulus. They are dome-shaped, measuring between 1.5 to 2 μm in length, and each participates in the following synaptic arrangement. When impressed into the surface of the P2

ending, F endings usually form two symmetrical to intermediate synapses: an axoaxonic synapse with the P2 ending and an axodendritic synapse with the central dendritic shaft that also receives an axodendritic synapse from the same P2 ending with which the F ending forms an axoaxonic synapse (Figures 7,13). Two other kinds of small axonal endings commonly enter the glomeruli. These include .5-1μm dome-shaped endings (R endings) containing small aggregates of large round (50-65 nm in diameter) synaptic vesicles. These endings are relatively sparse and form single asymmetrical axodendritic synapses on the central dendritic shaft that also receives a synapse from the P2 ending as well as a synapse from an F ending. The second type of small axonal ending is the r ending. They are few in number, smaller in size and are impressed into the surface of the central dendrite (Figures 7,13). The r endings measure 0.5-0.7 μm in length and contain a cluster of agranular small round (30 - 45 nm in diameter) synaptic vesicles at the lone asymmetrical synaptic junction formed by this terminal with the central dendrite.

DISCUSSION

The present anatomical study demonstrates that all four subdivisions of DM of rat Vo receive the terminal arborizations of two morphologically distinct types of primary trigeminal axons. Based on light and electron microscopic data, both types of axons are of the small myelinated variety. Previous light and electron microscopical analyses have shown that rat Vo receives two additional morphologically distinct types of small-diameter myelinated primary trigeminal axons (26). One type arborizes in VL and the other type terminates throughout BZ. The parent branches of the four groups of small myelinated axons terminating in Vo display the morphology and are in the size range generally accepted for Aσ primary axons (26). Based on previous electrophysiological data, these Aσ fibers most likely respond to light tactile and/or noxious stimuli from the orofacial region, (3,11,33,34,36,46,53,56, 59,60). Taken together these data suggest that within rat Vo there are at least four separate synaptic circuitries involved in the processing of orofacial pain and/or tactile input from small myelinated primary trigeminal axons. Two are located in DM with one each in BZ and VL. Autoradiographic, degeneration, and anterograde transganglionic HRP transport studies in the cat and rat agree that primary trigeminal axons terminate in Vo and are somatotopically organized (1,2,10,43,44,49,50,54,68,69). By comparing the locations of

the suggested subdivisions in rat Vo to the regions of termination of primary afferent axons belonging to branches associated with each of the three divisions of the rat trigeminal nerve (2,10,43,50), it can be concluded that DM would be receiving the terminal arborizations of a great many of the primary trigeminal neurons innervating mandibular orofacial receptive fields. Furthermore, DM also extends a short distance into the dorsal portion of the intermediate one-third of Vo, especially laterally. In this location, DM is in a position to receive terminal arbors of several of the primary trigeminal neurons whose peripheral processes course in branches of the maxillary division of the trigeminal nerve (43). The two HRP-labeled populations of small myelinated primary trigeminal axons analyzed in this study form their terminal arborizations throughout DM. Taken together, these data strongly suggest that the two populations of primary axons in this study are derived from primary trigeminal neurons whose peripheral receptive fields are located in orofacial regions (e.g. oral cavity) innervated by mandibular and maxillary divisions of the trigeminal nerve.

The findings of the present study suggest that at least two types of orofacial primary afferent input are being conveyed to neurons in all portions of DM. The primary endings from each of the two types of small-diameter primary trigeminal axons display differences in their cytology and synaptic relations. The single axodendritic synapse typical

of most of the P1 endings is in marked contrast to more complex glomerular synaptic arrangements involving the P2 endings. The synaptic arrangements of the primary endings in DM from both Type I and Type II primary afferents, are different from those of primary endings belonging to primary afferent axons terminating in glomeruli in other trigeminal sensory nuclei (28,29,30,31,40). However, the P2 ending does display a glomerular arrangement similar to that found for HRP-filled Primary endings in BZ belonging to unmyelinated primary trigeminal afferent axons (22). Primary endings of both Type I and Type II afferents make asymmetrical axodendritic synapses on a single dendritic shaft. According to previous ultrastructural studies (28,29,30,40) on synaptic circuitry in primary trigeminal afferent glomeruli, axodendritic synapses are the site where small-diameter primary axons deliver their inputs directly to the dendrites of second-order Vo neurons resulting in the activation of these cells. The neuronal origin of the dendritic elements cannot be determined absolutely, but the most likely sources are neurons whose dendrites are either confined to or enter DM where the two types of small-diameter primary axons form their terminal arborizations. The most probable neuronal sources or the dendrites in DM receiving Type I and Type II afferent input include trigeminocerebellar projection neurons located in the three portions of DM, (CDM, MDM, RDM; 26), as well as descending MDH projection neurons (18), trigeminospinal, SVN

and solitary projection neurons (64) and neurons projecting to Vmo, VII, and XII (65). In a previous study (22), distal dendritic shafts were occasionally found in VL glomeruli involving primary endings from small myelinated primary trigeminal axons, however, proximal dendritic shafts appeared to receive primary endings from Type I and Type II afferents in these studies. In addition, Type I and Type II primary endings did not synapse on dendritic spines. This is substantiated by information from Golgi and retrograde HRP studies (26) that show that the dendritic shafts of many DM neurons emit relatively few, widely scattered dendritic spines.

Non-primary axonal endings are components of small glomeruli in DM involving P2 endings and some P1 endings. However, synaptic vesicle-containing dendritic shafts and spines that have been observed in many primary afferent glomeruli in MDH (28,29) to be presynaptic to nonsynaptic vesicle-containing dendritic shafts and spines as well as to primary endings have not been observed in the glomeruli in these studies. Previous electron microscopic studies analyzing glomeruli involving PR endings from small myelinated axons in VL and BZ (22) have suggested that the transfer of input from the primary endings and the subsequent activation of second-order Vo neurons can be affected within each glomerulus by populations of axons from nonprimary neuronal sources. In this study the axons would be giving rise to the

P endings in some Type I glomeruli and the F endings in all Type II glomeruli. Their position and synaptic arrangement strongly suggests that both P and F endings play a major role in influencing small-diameter primary afferent transmission in DM. Both F and P endings exhibit symmetrical to intermediate synaptic contacts, thought to belong to axons derived from at least two sources that could inhibit or diminish the firing rate of second order Vo neurons in response to small-diameter primary input. In the case of the F endings, this would be accomplished either presynaptically through their axoaxonic synapses directly on the P2 endings and/or postsynaptically through their axodendritic synapses on the central dendritic shaft. In the case of the P ending this would be accomplished only presynaptically through their axoaxonic synapses directly in the P1 ending. Numerous studies have shown that terminals containing flattened synaptic vesicles like those observed in this study, which form similar synaptic connections around primary endings, are a common component of primary afferent glomeruli found in other trigeminal sensory nuclei and are probably derived from interneurons, (22,28, 29,40). Whether or not interneurons are present in DM has yet to be described.

Based on the above findings and the results of the present study most P1 endings probably transfer their small myelinated primary afferent input directly to second-order DM neurons without having it be affected by axons from nonprimary neuronal sources. In contrast, the transfer of small

myelinated primary afferent input from P2 endings to second order DM neurons most likely is affected substantially by at least one non-primary neuronal source. This Type I input reaches second order DM neurons unchanged from the periphery while Type II input to second order DM neurons undergoes significant modification before being relayed to other nuclei along the neuraxis.

Figure 1: Type I Primary Afferent Axon Terminal Arborizations

Composite drawings from horizontal sections showing the terminal arborizations in the dorsomedial (DM) subdivision ofrat trigeminal nucleus oralis (Vo) of one morphologically distinct type of HRP-filled primary trigeminal afferent axon (Type I). The parent fiber (P) travels caudally in the dorsomedial portion of the spinal trigeminal tract (SVT), entering Vo by traversing through the border zone subdivision (BZ) and terminating in DM as a long medially directed unbranched terminal strand, 425-650μm in length. Along the terminal strand (ts) are 14-33 irregularly spaced boutons (b) with one bouton always found at the terminal end of each strand. Bar = 10μm. Vmo, trigeminal motor nucleus; MDMv, middle ventral zone.

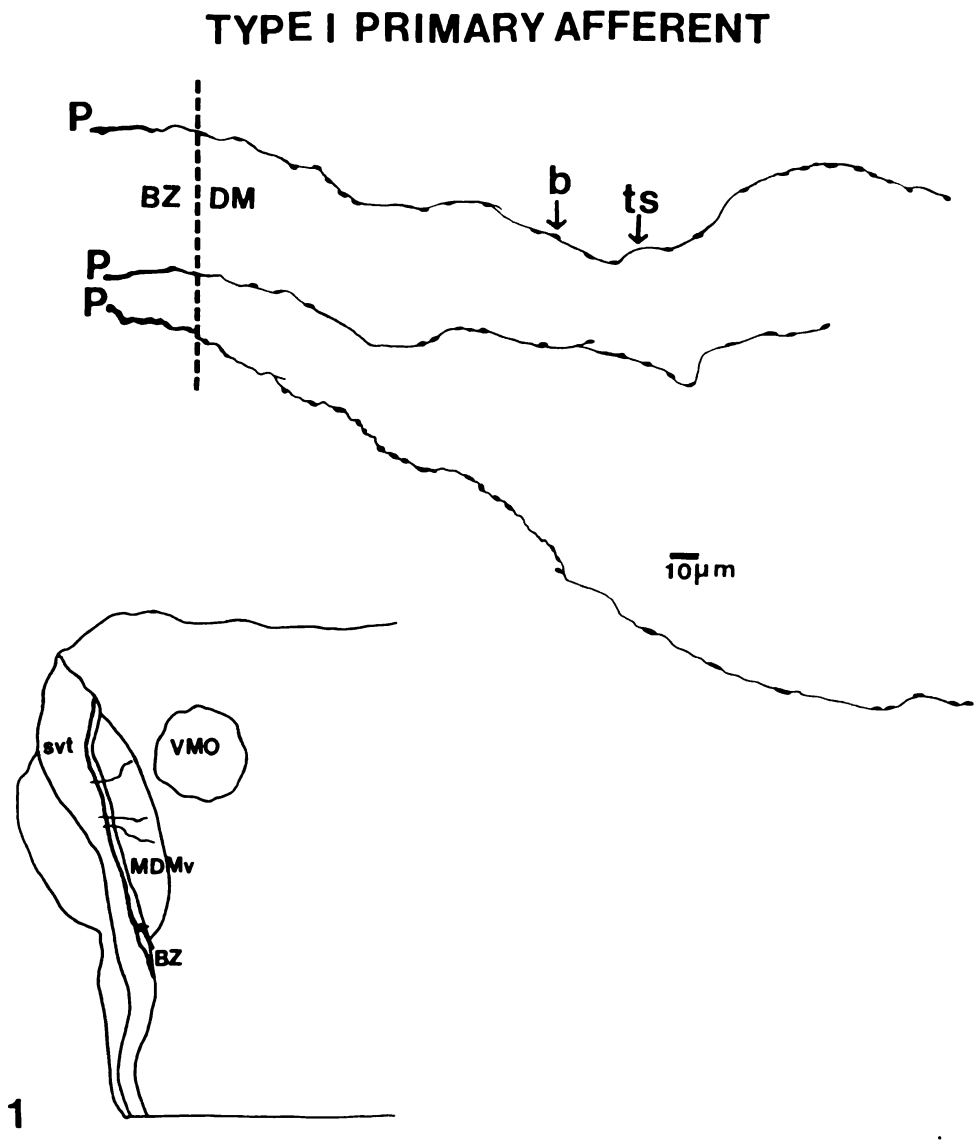

Figure 1

Figure 2: Type II Primary Afferent Axon Terminal Arborizations

Composite drawings from transverse sections showing the terminal arborizations in DM of rat Vo of the second morphologically distinct type of HRP-filled primary trigeminal afferent axon (Type II). Parent fibers are confined to and descend in dorsomedial SVT where they give rise to medially directed collaterals (C). These collaterals traverse BZ unbranched and enter DM dividing into two to four medially directed terminal strands (ts). Each strand extends from 28-74 μm in length. Along the terminal strand are 1-19 irregularly space boutons, with one always located at the terminal tip of each strand. Bar=10μm. VII, Facial motor nucleus; VL, ventrolateral subdivision; MDMd, middle dorsal zone.

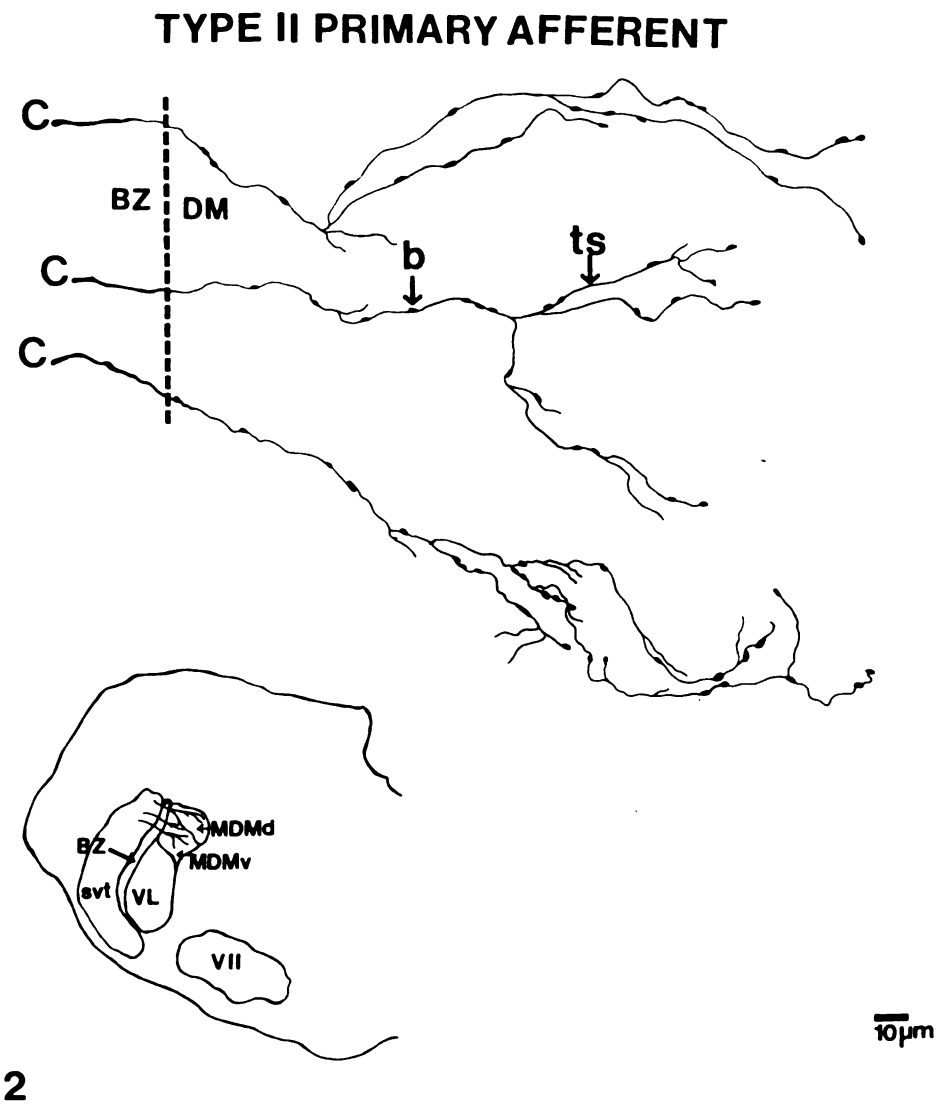
TYPE II PRIMARY AFFERENT
C
C
C
BZ
DM
b
ts
MDMd
MDMv
BZ
svt
VL
VII
10µm
2

Figure 2

Figure 3: Photomicrograph of Type II Primary Afferent

Photomicrograph that documents the morphological characteristics of the Type II primary afferent highlighting one of the terminal strands (ts) and one of the irregularly spaced boutons (b). x 1,824

Figure 4: Photomicrograph of Type I Primary Afferent

Photomicrograph that documents the morphological characteristics of the Type I primary afferent highlighting one of the terminal strands (ts) and one of the irregularly spaced boutons (b). x 1,686

Figure 5: Electron Micrograph of Type I and Type II Myelinated Parent Axons

Photomicrograph that documents the HRP labeled morphological characteristics of Type I and Type II parent fibers with their surrounding myelin sheaths in SVT. x 22,080

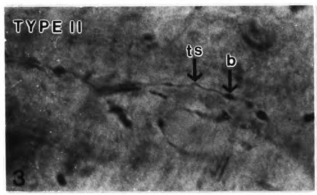

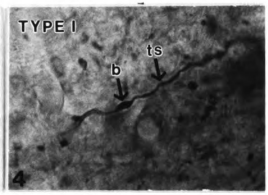

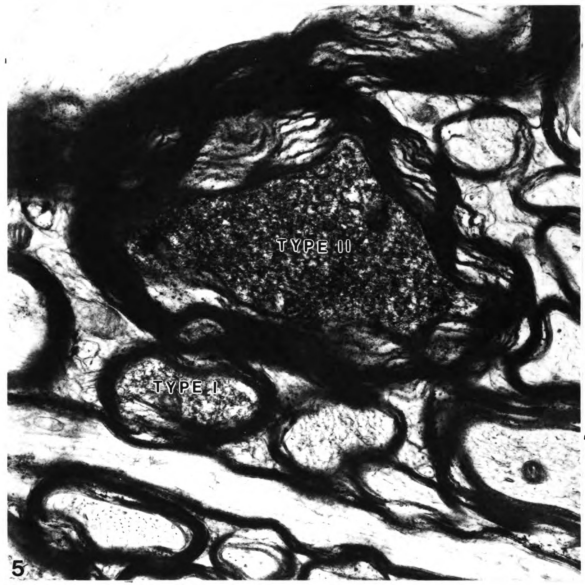

Figures 3, 4, 5

Figure 6: Diagram of Type I Axonal Endings and their Synaptic Connections

A schematic drawing taken from sets of serial thin sections (Figures 8,9,10) of the neuronal processes and synaptic connections in DM of Type I axonal endings. Primary axonal endings (P1) containing agranular synaptic vesicles form asymmetrical synaptic junctions with dendritic shafts (D). On occasion a P1 ending will be found in a simple glomerulus where it is postsynaptic to a single unlabeled axonal ending(P) making a symmetrical to intermediate synaptic junction and containing pleomorphic synaptic vesicles. Unlabeled axonal endings containing round (r) synaptic vesicles make asymmetrical axodendritic synapses with dendritic shafts. Appreciable portions of the Type I endings and their synaptic connections are surrounded by astrocytic processes (thick black lines). d, small dendritic shaft.

Figure 7: Diagram of Type II Axonal Ending and Their Synaptic Connections

A schematic drawing taken from sets of serial thin sections (Figures 11, 12, 13) of the neuronal processes and synaptic connections in DM Type II primary trigeminal afferent glomeruli. A primary axonal ending (P2) containing agranular synaptic vesicles and dense core vesicles forms an asymmetrical synaptic junction with a central dendritic shaft (D). Unlabeled axonal endings containing large (R) and small (r) round synaptic vesicles make asymmetrical axodendritic synapses with the central dendritic shaft. Unlabeled axonal endings containing flattened (F) synaptic vesicles form two symmetrical to intermediate synapses, an axoaxonic synapse with the P2 ending and an axodendritic synapse with the central dendritic shaft that also receives an axodendritic synapse from the same P2 ending with which the F ending forms an axoaxonic synapse. Appreciable portions of the glomerulus are surrounded by astrocytic processes (thick black lines).

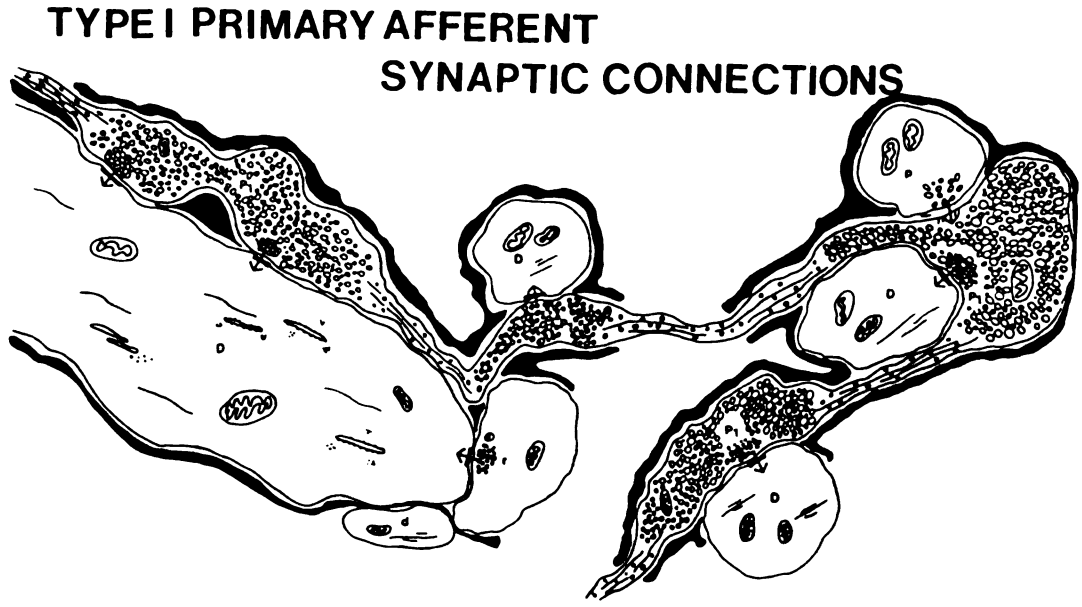

6

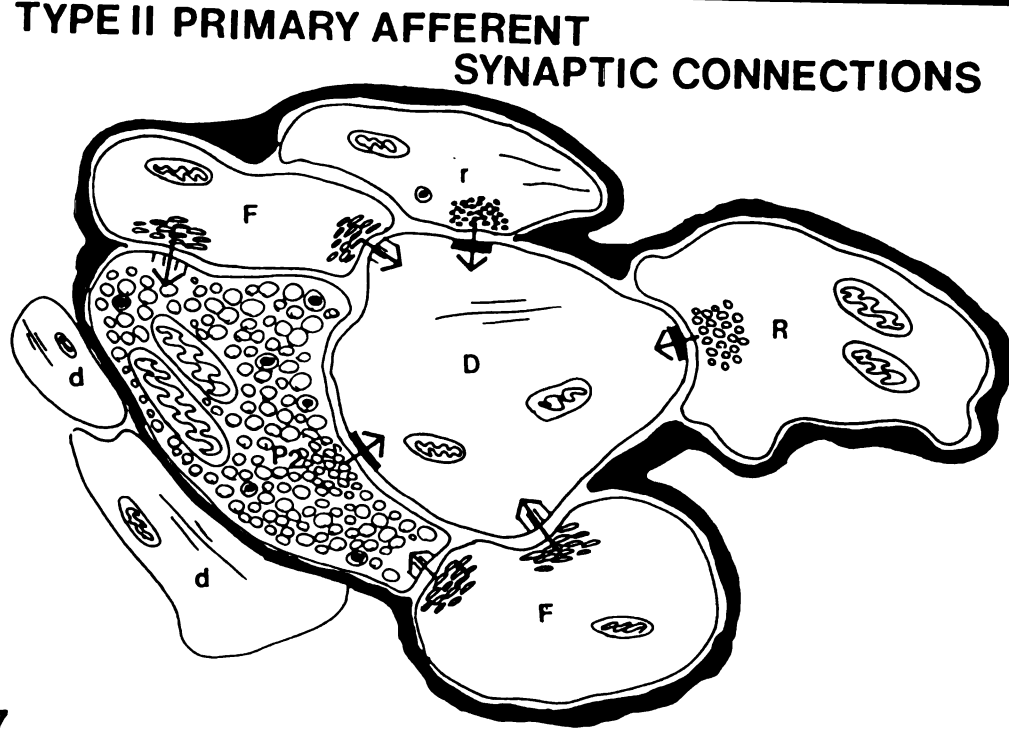

7

Figures 6,7

Figure 8: Electron Micrograph of Type I Axonal Ending and Its Synaptic Connections

Two P1 endings surrounded by glial processes, suggest formation of asymmetrical synapses (arrows) on the adjacent dendritic shaft (D). ts, terminal strand; x 52,250

Figure 9: Electron Micrograph of Type I Axonal Ending and Its Synaptic Connections

A dome-shaped P1 ending wrapping around a dendritic shaft (D) and forming an asymmetrical axodendritic synapse (arrow). An unlabeled axonal ending with small round (r) synaptic vesicles also synapses on the dendrite, D, by forming an asymmetrical synapse (arrow). x 52,250

Figure 10: Electron Micrograph of Type I Axonal Ending and Its Synaptic Connections

On occasion a P1 ending will be found in a simple glomerulus where it is postsynaptic to a single unlabeled axonal ending (p). The p endings form symmetrical to intermediate synaptic junctions (arrow) and contain pleomorphic synaptic vesicles. x 52,250

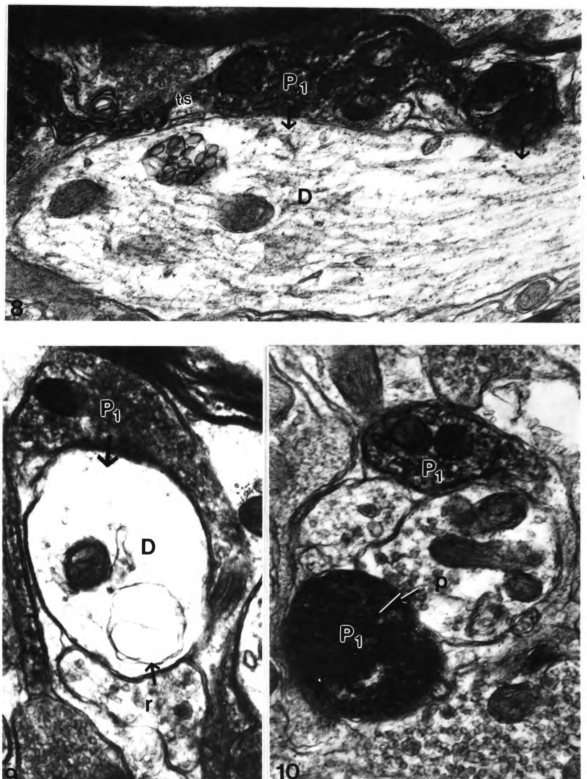

Figures 8, 9, 10

Figure 11: Electron Micrograph of Type II Axonal Ending and Its Synaptic Connections

Representative thin section through a P2 axonal ending in the DM neuropil containing agranular spherical synaptic vesicles among which are scattered several dense core vesicles (DCV). The P2 ending probably synapses (arrow) on the adjacent dendritic shaft (D). x 48,460

Figure 12: Electron Micrograph of Type II Axonal Ending and Its Synaptic Connections

A glomerulus is formed by a central dendritic shaft (D) and multiple surrounding neuronal processes. The P2 axonal ending forms an asymmetrical synapse (arrow) with the central dendrite. An unlabeled axonal ending with large round (R) synaptic vesicles also synapses on the central dendrite by forming an asymmetrical synapse (arrow). x 34,920

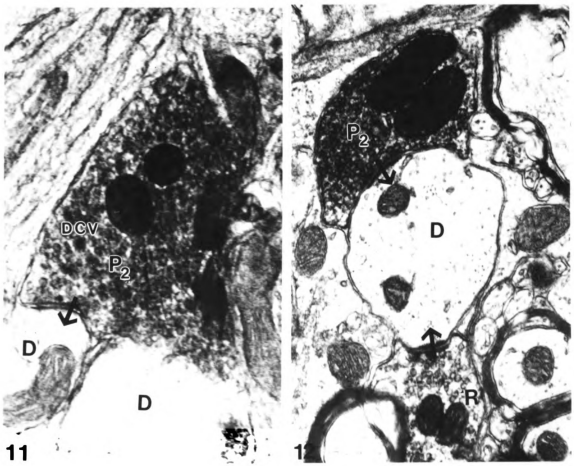

Figures 11, 12

Figure 13a,b,c,d: Electron Micrographs Taken From Serial Sections Through a Type II Axonal Ending and Its Synaptic Connections

Serial sections through a glomerulus showing the P2 axonal ending and its asymmetrical synapse (arrow) on a central dendrite (D). Multiple surrounding neuronal processes are clearly demonstrated. An unlabeled axonal ending with small round (r) synaptic vesicles forms an asymmetrical synapse (arrow) with the central dendrite. Two unlabeled axonal endings, each containing flattened (F) synaptic vesicles, form two symmetrical to intermediate synaptic junctions, one on the central dendrite and the other on the P2 ending. x 34,920

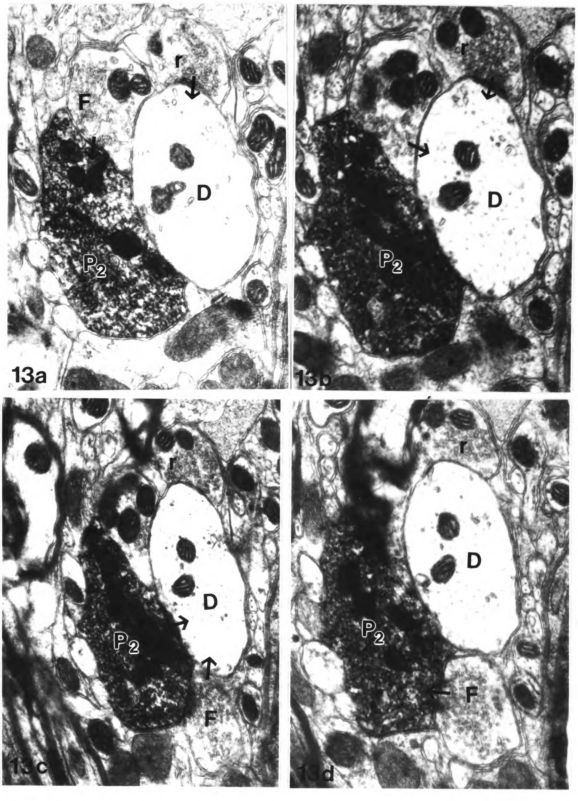

Figure 13

BIBLIOGRAPHY

1. Arvidsson, J. and Gobel, S. (1981) An HRP study of the central projections of primary trigeminal neurons which innervate tooth pulps in the cat. Brain Res., 210:1-16.

2. Arvidsson, J. and G. Grant, (1978) Further observations on transganglionic degeneration in trigeminal primary sensory neurons. Brain Res. 4:1-12.

3. Azerad, J., Woda, A., and Albe-Fessard, D. (1982) Physiological properties of neurons in different parts of the cat trigeminal sensory complex. Brain Res. 246:7-21.

4. Belford, G. R. and H. P. Killackey. (1979) Vibrissae representation in subcortical trigeminal centers of the neonatal rat. J. of Comp. Neurol. 183:305-322.

5. Bernardo, K. L., M.M. Pokay, and T. A. Woolsey. (1986) In vitro labeling of axonal projections in the mammalian central nervous system. J. of Neurol. Methods. 16:89-101.

6. Broton, J. G., J. W. Hu, and B J. Sessle. (1988) Effects of temporomandibular joint stimulation on nociceptive and non-nociceptive neurons of the cat's trigeminal subnucleus caudalis (medullary dorsal horn). J. Neurophysiol. 59:1575-1589.

7. Broton, J. G. and J. Rosenfeld. (1985) Effects of trigeminal tractotomy on facial thermal nociception in the rat. Brain Res. 333:63-72.

8. Bruce, L. L., J. G. Mchaffie and B. E. Stein (1987) The organization of trigeminotectal and trigeminothalamic neurons in rodents: A double-labeling study with fluorescent dyes. J. Comp. Neurol. 262:315-530.

9. Capra, N. F. (1987) Localization and central projections of primary afferent neurons that innervate the temporomandibular joint in cats. Somatosensory Res. 4:201- 213.

10. Contreras, R. J., R. M. Beckstead and R. Norgren. (1982) The central projections of the trigeminal, facial,glossopharyngeal and vagus nerves: an autoradiographic study in the rat. J. of the Autonomic Ner. Sys. 6:303-322.

11. Darian-Smith I. (1973) The trigeminal system. In:Handbook of Sensory Physiology. Vol II. A. Iggo, ed. Springer-Verlag, Berlin, pp. 271-314.

12. Erzurumlu, R. S., and H. P. Killackey (1979) Efferent connections of the brainstem trigeminal complex with the facial nucleus of the rat. J. Comp. Neurol. 188:75-86.

13. Erzurumlu, R. S., C. A. Bates, and H. P. Killackey(1980) Differential organization of thalamic projection cells in the brain stem trigeminal complex of the rat. Brain Res. 198:427-433.

14. Falls, W. M. (1983a) A Golgi type II neuron in trigeminal nucleus oralis: A Golgi study in the rat. Neurosci. Letts. 41:11-7.

15. Falls, W. M. (1983b) Light and EM analysis of identified trigeminospinal projection neurons in rat trigeminal nucleus oralis. Anat. Rec. 205:55A.

16. Falls, W. M. (1984a) Termination in trigeminal nucleus oralis of ascending intratrigeminal axons originating from neurons in the medullary dorsal horn: An HRP study employing light and electron microscopy. Brain Res. 29:136-140

17. Falls, W. M. (1984b) Axonal endings terminating on dendrite of identified large trigeminospinal projection neurons in rat trigeminal nucleus oralis. Brain Res. 324:335-341.

18. Falls, W. M. (1984c) The morphology of neurons in trigeminal nucleus oralis projecting to the medullary dorsal horn (trigeminal nucleus caudalis): A retrograde HRP and golgi study. Neuroscience 13:1279-1298.

19. Falls, W. M. (1986a) Morphology and synaptic connections of unmyelinated primary axons in the border zone of rat trigeminal nucleus oralis. Neurosci. Letts. 70:342-347.

20. Falls, W. M. (1986b) Morphology and synaptic connections of myelinated primary axons in the ventrolateral portion of rat trigeminal nucleus oralis. J. Comp. Neurol. 244:96-110.

21. Falls, W. M. (1987) Direct connections of primary trigeminal afferent axons with trigeminocerebellar projection neurons in the border zone of rat trigeminal nucleus oralis. Neurosci. Letts. 83:247-252.

22. Falls, W. M. (1988) The synaptic organization of trigeminal primary axons in nucleus oralis. J. Electron Microscopy Tech. 10:213-227.

23. Falls, W. M. and M. M. Alban. (1986a) Morphological features of identified trigeminocerebellar projection neurons in the border zone of rat trigeminal nucleus oralis. Somatosensory Res. 4:1-12.

24. Falls, W. M. and M. M. Alban. (1986b) Morphology and synaptic connections of small myelinated primary trigeminal axons arborizing among neurons in the border zone of rat trigeminal nucleus oralis. Somatosensory Res. 4:97-110.

25. Falls, W.M., B.J. Moore, and M.T. Schneider. (1990) Fine structural characteristics and synaptic connections of trigeminocerebellar projection neurons in rat trigeminal nucleus oralis. Somatosensory and Motor Res. 7:1-18.

26. Falls, W. M., R. E. Rice and J. P. Van Wagner. (1985) The dorsomedial portion of trigeminal nucleus oralis (Vo) in the rat: cytology and projections to the cerebellum. Somatosensory Res. 3:89-118.

27. Fukushima, T., and F. W. L. Kerr (1979) Organization of trigeminothalamic tracts and other thalamic afferent systems of the brainstem in rat: presence of gelatinosa neurons with thalamic connections. J. Comp. Neurol. 183:169-184.

28. Gobel, S. (1974) Synaptic Organization of the substantia gelatinosa glomeruli in the spinal trigeminal nucleus of the adult cat. J. Neurocytol., 3:219-243.

29. Gobel, S. (1976a) Dendroaxonic synapses in the substantia gelatinosa glomeruli of the spinal trigeminal nucleus of the cat. J. Comp. Neurol., 167:165-176.

30. Gobel, S. (1976b) Principles of organization in the substantia gelatinosa layer of the spinal trigeminal nucleus. In: Advances in Pain Research and Therapy, Vol I, J.J. Bonica and D. Albe-Fessaard, eds. Raven Press, New York, pp. 165-170.

31. Gobel, S. and Dubner, R. (1969) Fine structural studies of the main sensory trigeminal nucleus in the cat and rat. J. Comp, Neurol., 137:459-494.

32. Gobel, S., W. M. Falls, and S. Hockfield (1977). The division of the dorsal and ventral horns of the mammalian caudal medulla into eight layers using anatomical critieria. In: Pain in the Trigeminal region. D. J. Anderson, and B. Matthews (eds.) Amsterdam: Elsevier/ North-Holland. pp. 443-453.

33. Greenwood, F. (1973) An electrophysiological study of the central connections for primary afferent fibers from the dental pulp in the cat. Arch. Oral Biol., 17:701-709.

34. Hayashi, H. (1982) Differential terminal distribution of single large cutaneous afferent fibers in the spinal trigeminal nucleus and in the cervical spinal dorsal horn. Brain Res., 244:173-177.

35. Hayashi, H. (1985) Morphology of terminations of small and large myelinated trigeminal primary afferent fibers in the cat. J. of Comp. Neurol. 240:71-89.

36. Hayashi, H., R. Sumino and B. J. Sessle (1984) Functional organization of trigeminal subnucleus interpolaris: Nociceptive and innocuous afferent inputs, projections to thalamus, cerebellum, and spinal cord, and descending modulation from periaqueductal gray. J. Neurophysiol. 51:890-905.

37. Hockfield, S. and S. Gobel (1978) Neurons in and near nucleus caudalis with long ascending projection axons demonstrated by retrograde labeling with horseradish peroxidase. Brain Res. 204:415-420.

38. Hoffman, D. S., R. Dubner, R. L. Hayes, and T. P. Medlin (1981) Neuronal activity in medullary dorsal horn of awake monkeys trained in a thermal discrimination task. I. Responses to innocuous and noxious thermal stimuli. J. Neurophysiol. 46:409-427.

39. Huerta, M. F. A. Frankfurter, and J. K. Harding (1983) Studies of the principal sensory and spinal trigeminal nuclei of the rat: projections to the superior colliculus, inferior olive and cerebellum. J. Comp. Neurol. 220:147-167.

40. Ide, L.S. and Killackey, H.P. (1985) Fine structural survey of the rat's brainstem sensory trigeminal complex. J. Comp. Neurol., 235:145-168.

41. Ishidori, H., T. Nishimori, Y. Shigenaga, S. Suemune, Y. Dateoka, M. Sera and N. Nagasaka. (1986) Representation of upper and lower primary teeth in the trigeminal sensory nuclear complex in the young dog. Brain Res. 370:153-158.

42. Itoh, K., A. Konishi, S. Nomua, N. Mizuno, Y. Nakamura, and T. Sugimoto. (1979) Application of coupled oxidation reaction to electron microscopic demonstration of horseradish peroxidase: Cobalt-glucose oxidase method. Brain Res. 175: 341-346.

43. Jacquin, M. F., K. Semba, M. D. Egger, and R. W. Rhoades. (1983) Organization of HRP-labeled trigeminal mandibular primary afferent neurons in the rat. J. of Comp. Neurol. 215:397-420.

44. Jacquin, Mark F. K. Semba, R. W. Rhoades, and M. David Egger. (1982). Trigeminal primary afferents project bilaterally to dorsal horn and ipsilaterally to cerebellum, reticular formation, and cuneate, solitary, supratrigeminal and vagal nuclei. Brain Res. 246:285-291.

45. Keller, O., M. Kalina, E. Ujec, A. Zivnand L. Vyklicky (1981) Projection of tooth pulp afferents to the brainstem and the cortex in the cat. Neuro. Letts. 25:233-237.

46. Khayyat, G.F., Yu. Y.J. and King, R. B. (1975) Response patterns to noxious and non-noxious stimuli in rostral trigeminal nuclei. Brain Res., 97:47-60.

47. Leong, S. K., J. Y. Shieh and W. C. Wong (1984) Localizing spinal-cord-projecting neurons in adult albino rats. J. Comp. Neurol. 228:1-17.

48. Liu, D. and Y. Hu (1988) The central projection of the great auricular nerve primary afferent fibers -- an HRP transganglionic tracing method. Brain Res. 445: 205-210.

49. Marfurt, C. F. (1981) The central projections of trigeminal primary afferent neurons in the cat as determined by transganglionic transport of horseradish peroxidase. J. of Comp. Neurol. 203:785-798.

50. Marfurt, C. F. and D. F. Turner (1984) The central projections of tooth pulp afferent neurons in the rat as determined by the transganglionic transport of horseradish peroxidase. J. of Comp. Neuro. 223:535-547.

51. Marfurt, C. F. and S. F. Echtenkamp (1988) Central projections and trigeminal ganglion location of corneal afferent neurons in the monkey, Macaca fascicularis. J. of Comp. Neuro. 272:370-382.

52. NIH Guide for the Care and Use of Laboratory Animals. NIH, 9000 Rockville Pike, Bethesda, MD. 20892, 1985.

53. Nord, S. G. (1976) Response of neurons in rostral and caudal trigeminal nuclei to tooth pulp stimulation. Brain Res. Bull., 1:489-492.

54. Panneton, W. M. and H. Burton. (1981) Corneal and periocular representation within the trigeminal sensory complex in the cat studied with transganglionic transport of horseradish peroxidase. J. of Comp. Neurol. 199:327-344.

55. Paxinos, G. and C. Watson (1986) The Rat Brain Sterotaxic Coordinates 2d Edition. New York.

56. Rowe, M. J. and Sessle, B.J. (1972) Responses of trigeminal ganglion and brain stem neurons in the cat to mechanical and thermal stimulation of the face. Brain Res., 42:367-384.

57. Ruggiero, D. A., C. A. Ross and D. J. Reis (1981) Projections from the spinal trigeminal nucleus to the entire length of the spinal cord in the rat. Brain Res. 23265:225-233.

58. Sessle, B. J. (1987) The neurobiology of facial and dental pain: present knowledge, future directions. J. Dent. Res. 66:962-981.

59. Sessle, B. J. and Greenwood, L. F. (1976) Inputs to trigeminal brain stem neurones from facial, oral, tooth pulp and pharyngolaryngeal tissues. I. Responses to innocuous and noxious stimuli. Brain Res., 117:211-226.

60. Sessle, B.J. and Hu, J.W. (1981) Raphe-induced suppression of the jaw-opening reflex and single neurons in trigeminal subnucleus oralis, and influence of naloxone and subnucleus caudalis, Pain, 10:19-36.

61. Shigenaga, Y., T. Okamoto, T. Nishimori, S. Suemune, I.D. Nasution, I.C. Chen, K. Tsuru, A. Yoshida, K. Tabuchi, M. Hosoi, and H. Tsuru. (1986a). Oral and facial representation in the trigeminal principal and rostral spinal nuclei of the cat. J. Comp. Neurol. 244:1-18.

62. Shigenaga, Y., S. Suemune, M. Nishimura, T. Nishimori, H. Sato, H. Ishidori, A. Yoshida, K. Tsuru, Y. Tsuiki, Y. Dateoka, I.D. Nasution, and M. Hosoi. (1986b) Topographic representation of lower and upper teeth within the trigeminal sensory nuclei of adult cat as demonstrated by the transganglionic transport of horseradish peroxidase. J. Comp. Neurol. 251:299-316.

63. Silverman, J. D., and L. Kruger (1985) Projections of the rat trigeminal sensory nuclear complex demonstrated by multiple fluorescent dye retrograde transport. Brain Res. 361:383-388.

64. Smith, L.A. and Falls, W.M. (1994) Topographical Distribution and Morphological Features of Second Order Projections from identified subdivisional Areas of Rat Trigeminal Nucleus Oralis. Ph.D. Thesis. Dept. of Anatomy, Michigan State University, East Lansing, MI.

65. Sohn, D.J. and Falls, W.M. (1994) Comparison of the Distribution and Morphology of Neurons in Rat Trigeminal Nucleus Oralis Projecting to Facial, Hypoglossal and Trigeminal Motor Nuclei. Ph.D. Thesis. Dept. of Anatomy. Michigan State University, East Lansing, MI.

66. Sugimoto, T. and M. Takemura. (1993) Tooth Pulp Primary Neurons: Cell Size Analysis, Central Connnection, and Carbonic Anhydrase Activity. Brain Research Bulletin. 30:221-226.

67. Travers, J. and Norgren, R., (1983) Afferent projections to the oral motor nuclei in the rat. J. Comp. Neurol., 220:280-298.

68. Westrum L.E., Candfield, R.C., and O'Connor, T.A. (1980) Projections from dental structures to the brain stem trigeminal complex as shown by transganglionic transport of horseradish peroxidase. Neurosci. Lett., 20:31-36.

69. Westrum, L. E., R. C. Canfield and T. A. O'Connor. (1981) Each canine tooth projects to all brain stem trigeminal nuclei in cat. Exper. Neurol. 74:787-799.

CHAPTER II

COMPARISON OF THE DISTRIBUTION AND MORPHOLOGY OF NEURONS IN RAT TRIGEMINAL NUCLEUS ORALIS PROJECTING TO FACIAL, HYPOGLOSSAL AND TRIGEMINAL MOTOR NUCLEI

INTRODUCTION

Trigeminal nucleus oralis (Vo), the most rostral subdivision of the mammalian spinal trigeminal nucleus (SVN), is thought to play a major role in the overall circuitry underlying orofacial function, dysfunction and reflexes (e.g. corneal reflex, orienting reflex, pinnae orienting reflex, jaw-opening reflex, etc.). Vo is considered a significant contributor to the reception, central processing, modification and relay of nociceptive and mechanoreceptive information from the facial skin, oral and nasal cavities, temporomandibular joint, cornea and tooth pulp. These activities suggest that Vo may play an important role in numerous acute and chronic pain states (e.g. trigeminal neuralgia). On the basis of several morphological and functional criteria, rat Vo can be divided into three subdivisions: ventrolateral (VL), dorsomedial (DM), and border zone (BZ), (6,8,9,10,14,15,26).

Each Vo subdivision has been shown to receive morphologically and functionally distinct groups of primary

and non-primary afferent axons which are in a position to directly influence the activity of second order Vo projection neurons (8,11,12,14,15,26,45). These neurons have most of their dendritic arbors confined to the subdivision and thus provide the efferent outflow from each Vo subdivision affecting the synaptic activity within numerous locations along the neuraxis.

Retrograde transport studies in the rat (10) and cat (31)have shown that VL contains three morphologically distinct types of small neurons which project to medullary dorsal horn (MDH). In addition, VL trigeminospinal projection neurons innervate all levels of the rat spinal cord (9,34,40). Trigeminofacial projection neurons (4,5); trigeminothalamic projection neurons, and(3,5,27,43); trigeminotectal projection neurons (3,32), have also been shown to be present in VL. Anterograde studies utilizing phaseolus vulgaris leucoagglutinin (PHA-L) have shown that injections into rat VL result in labeled terminal axonal arbors in the cervical and thoracic spinal cord, cerebellum, thalamus, solitary nucleus, and SVN bilaterally (44). Anterograde studies have revealed that after PHA-L injections into BZ, labeling of terminal axonal arbors was found in cervical and thoracic spinal cord, cerebellum, and thalamus, as well as, solitary nucleus and SVN bilaterally (44). Retrograde studies have shown a variety of projection neurons to be present in BZ. A single population of trigeminocerebellar projection neurons is

situated in the dorsal portion of BZ, (14) as well as descending MDH projection neurons (8) located in the ventral portion. Small populations of morphologically distinct trigeminotectal (3), trigeminospinal, (9), and trigeminothalamic (3)projection neurons are also found throughout BZ.

Within DM, utilizing the retrograde horseradish peroxidase (HRP) method, five morphologically distinct types of trigeminocerebellar projection neurons have been identified, all of which innervate one or more of the orofacial portions of four major tactile areas in the rat cerebellar cortex (26). Injections of PHA-L into DM anterogradely labeled terminal axonal arbors at all levels of the rat spinal cord, in the thalamus, solitary nucleus, bilateral SVN, as well as oculomotor (III), trochlear (IV) and abducens (VI) cranial nerve nuclei and the Edinger-Westphal nucleus (44).

Of particular interest are the efferent projections from Vo neurons to the cranial nerve motor nuclei, as these neurons are believed to provide a route for Vo involvement in complex reflexes (e.g. corneal reflex) elicited by stimulation of the skin of the face, oral and nasal mucous membranes and muscles, tendons and bones of the jaw and face. Presently, information is lacking on the precise distribution, density and morphology of these projection neurons in relation to Vo subdivisions. In a recent anterograde PHA-L study in the rat, the overall

pattern, organization and morphology of efferent axons arising from projection neurons in each Vo subdivision and forming terminal axonal arborizations in trigeminal (Vmo), facial (VII), and hypoglossal (XII) motor nuclei were examined (44). Following injections into DM and VL, labeled axons and terminal arbors were observed bilaterally in VII, XII and Vmo. Injections confined to BZ produced labeling of axons and terminal arbors ipsilaterally in Vmo and bilaterally in VII.

The results of this study (44) suggest that each subdivision of rat Vo may be capable of influencing motor output from these cranial nerve nuclei. The terminal arbors of Vo efferents in Vmo, VII and XII were morphologically different suggesting that different populations of Vo neurons project to each nucleus. In Vmo, a single population of efferent axons was found. In VII, two morphologically distinct types of Vo efferent terminal axonal arborizations were noted. Two morphologically distinct populations of efferent axons were also seen to terminate in XII. Furthermore, at least four of these five types of terminal axonal arbors were morphologically distinct from each other. The present light microscopic study continues to examine the efferent connections of projection neurons in Vo subdivisions to Vmo, VII, and XII. Utilizing the retrograde HRP technique, regional distribution and morphology of labeled trigeminofacial, trigeminohypoglossal and trigeminomotor neurons in rat Vo is examined and compared following

injections of HRP into Vmo, VII and XII. The density, distribution and somatodendritic morphology, when evident of these neurons is evaluated and compared throughout the rostrocaudal extent of Vo.

MATERIALS AND METHODS

Six adult male Sprague Dawley albino rats (250-300 g) were anesthetized with sodium pentobarbital (35-40 mg/kg)and positioned in a stereotaxic apparatus (Kopf). Aseptic technique was employed for all surgeries. The scalp was incised and a small opening was made in the cranium overlying the cerebellar cortex (cases #1-4) and in the left parietal bone (cases #5-6). The dural sheath was incised. A 0.05% solution of HRP (0.0005 g HRP in 10 μl 0.9% saline) was placed in a glass micropipette (inside tip diameter 20-30 μm) and iontophoretically delivered by a pulsed (7 seconds on, 7 seconds off) positive current of 5 mA (Midgard, Transkinetics model CS3) into either VII, XII, or Vmo utilizing coordinates obtained from the stereotaxic atlas of Paxinos and Watson('86). Injections were made at an angle of approximately 90°, with respect to the horizontal plane, for VII and XII and an angle of approximately 78°' with respect to the horizontal plane, for Vmo. Following termination of the current, the micropipette was left in place for an additional 5 minutes and then withdrawn. Upon completion of the experiment, gelfoam (UpJohn Company) was positioned in the opening, the incision was clamped closed, and an application of triple antibiotic ointment (Rugby Laboratories) was placed over the incision site. All animals were housed, maintained and cared for according to federally prescribed guidelines (38).

Forty-eight hours later, the animals were perfused according to the procedure described previously (Chapter 1). Sections of the brainstem containing the trigeminal sensory nuclear complex (TSNC) were blocked and sectioned on an Oxford Vibratome into 50μm thick sections in the transverse plane. Procedures for processing the tissue for HRP activity utilizing the cobalt-glucose oxidase method as well as section preparation for initial light microscopic examination has been described previously in Chapter 1. The full extent of the injection site was determined under brightfield illumination. Representative camera lucida drawings and photomicrographs (25X objective) of HRP-filled target sites were made(Figures 1a,b,c; 2a,b,c). In order to preserve relative cell morphology, the positions of retrogradely labeled neurons within Vo were plotted from serial sections throughout the rostrocaudal extent of the nucleus using a drawing tube and a 40X objective attached to a Leitz Laborlux 12 microscope (Figures 3,4,5). Retrogradely labeled neurons were identified by their content of HRP granules distributed throughout the cytoplasm. Only those profiles exhibiting a distinct nucleus were plotted. Camera lucida drawings of individual retrogradely labeled neurons throughout the rostrocaudal extent of the nucleus were made using a 40X objective (Figures 9, 10, 11). Photomicrographs of representative retrogradely labeled neurons from each subdivision were taken at 40X (Figures 9,10,11). The somatic cross-sectional areas of

retrogradely labeled neurons were measured using a Bioquant Image Analysis System which computed these areas from tracings of the perimeters of labeled neurons drawn with the aid of a camera lucida using a 40X objective. Retrogradely labeled neurons were grouped according to their position within the various cytoarchitecturally distinct Vo subdivisions defined in previous studies (7,8,11,12,13,14,15,26). These measurements were grouped into block intervals of 25 μm^2 and plotted as frequency histograms for each of the proposed subdivisions (Figures 13, 14) and used for the compilation of the total somatic cross-sectional area histograms (Figure 12). The mean and standard deviations were calculated for all sets of data. Relative frequencies of labeling of specific projection neurons were generated from the number of cells measured in each region. Histograms were drawn using Freelance Graphics on IBM-PC.

RESULTS

Following unilateral HRP injections into Vmo, VII, and XII motor nuclei, the morphology and distribution of retrogradely labeled trigeminomotor, trigeminofacial, and trigeminohypoglossal projection neurons were examined throughout the rostrocaudal extent of Vo, bilaterally. In each case, the intranuclear regional distribution of labeled neurons was plotted and illustrated (Figures 3,4,5) by a series of selected line drawings taken from four representative coronal sections through rat Vo relative to the regions of DM, one section each through rostral (RDM) and caudal (CDM) DM and two sections through middle (MDM) DM. Vo extends from the caudal pole of VII where it exhibits an overlap with trigeminal nucleus interpolaris (Vi), to the rostral pole of VII, where it gradually overlaps with the main sensory trigeminal nucleus (Vms). All three Vo subdivisions extend the entire rostrocaudal length of the nucleus. BZ is a long, thin subdivision located along the lateral border of the nucleus, immediately adjacent to SVT. VL is located medial to the ventral two-thirds of BZ, and occupies the largest area of the nucleus. DM is located dorsal to VL and medial to the dorsal one-third of BZ.

NEURONS PROJECTING TO THE TRIGEMINAL MOTOR NUCLEUS

Unilateral HRP deposits were localized within Vmo (Figure 1a). The schematic diagram in Figure 2a shows the locations of

two injection sites in two different animals in Vmo and the extent of overlap. The photomicrograph in Figure 1a illustrates the spread of HRP in one of the animals following a single injection centered in Vmo. This injection filled the majority of the rostro-caudal extent of the nucleus while filling three-fourths of the dorsal-ventral extent. It occupies an area measuring 1,335μm rostrocaudally, 1,120μm dorsoventrally and 1,160μm mediolaterally. The injection in the second animal is somewhat larger than in first animal. The nucleus is almost filled completely with reaction product with some spread into the neighboring peritrigeminal and intertrigeminal nuclei. The injection site occupies an area measuring 1,500μm rostrocaudally, 1,360μm dorsoventrally and 1,240μm mediolaterally.

Figure 3 is series of line drawings from coronal sections through the brainstem containing Vo showing the location of retrogradely labeled neurons as a result of HRP injection into Vmo in the second animal. One hundred twenty-two neurons are filled with HRP reaction product. The majority of labeled Vmo neurons are located in ipsilateral VL and DM regions with a few labeled cells in BZ. Contralaterally, DM contains two labeled neurons. Although labeled neurons were found throughout the rostrocaudal extent of Vo, approximately two-thirds were located in the middle one-third of the nucleus with the other one-third of labeled cells found near the rostral and caudal poles of Vo. The rostral pole of Vo

contained the least number of labeled neurons. Labeled VL neurons outnumbered those in DM by a 2:1 ratio.

Two major types of retrogradely labeled trigeminomotor projection neurons were found in VL and DM (Figures 6,9). The cell bodies of these neurons were basically spherical in shape with a few pyramidal-shaped neurons scattered throughout VL. The labeled cells could be grouped into small (< 25μm in diameter) and large (>25 μm) varieties with somatic cross-sectional areas of <300μm^2 and >300μm^2, respectively. Their average cross-sectional areas were 175μm^2 for the small cells and 407μm^2 for the large neurons. (Figures 13,14).

The vast majority of labeled neurons belonged to the small cell population. Although each Vo subdivision contained both populations of neurons, large size cells were found more frequently in VL, while small size neurons predominated in DM. The average cross-sectional area of large and small labeled cells in VL were 145μm^2 and 425μm^2, respectively, while the average cross-sectional area of large and small labeled cells in DM were 225μm^2 and 442μm^2, respectively. At the caudal pole of Vo, labeled neurons were located almost exclusively in the medial one-half of both DM and VL. Only one neuron was found in dorsal BZ. There were no labeled neurons found in the caudal pole of contralateral Vo. All of the labeled neurons belonged to the small cell population and had spherical somata. A few small, pyramidal shaped neurons were found in VL. Portions of the dendritic fields were visible on the most

densely filled neurons. DM neurons presented a bipolar appearance while those cells in VL had thin radiating dendrites or a bipolar appearance (Figures 6,9). The number of labeled neurons increased in the middle one-third of Vo, both in DM and VL (Figure 3). BZ continued to show very few labeled neurons and they were generally located in its ventral half. Contralateral DM also contained a few labeled small cells. Moving from caudal to rostral, labeled neurons were most prominent in the medial one-half of Vo caudally, and the lateral one-half rostrally. Labeled neurons were most dense dorsally in DM and ventrally in VL leaving a conspicuous absence of neurons ventrally in DM and dorsally in VL. Some labeled DM and VL neurons were small bipolar-shaped cells with spherical shaped cell bodies, while, a number of large size neurons with spherical shaped somata were present in DM and VL, as well as a few pyramidal-shaped cell bodies in VL. Neurons with bipolar-shaped dendritic fields were observed in DM while neurons with multipolar-shaped dendritic fields were present in both VL and DM (Figures 6,9).

At the rostral pole of Vo there was a striking paucity of labeled neurons (Figure 3). Of the few cells present in VL, most had large spherical-shaped somata while those scattered cells in DM possessed small spherical-shaped cell bodies. Neurons in both subdivisions appeared to have more bipolar-shaped dendritic fields (Figures 6,9). There were no labeled neurons found in BZ and the rostral pole of Vo

contralaterally contained no labeled cells.

NEURONS PROJECTING TO FACIAL MOTOR NUCLEUS

Unilateral HRP injections were made in VII in two animals. The schematic diagram in Figure 2b illustrates the two injection sites and the spread of HRP in each while the photomicrograph in Figure 1b illustrates the spread of HRP in the second animal. This injection site measures 1,300μm rostrocaudally, 1,080μm dorsoventrally and 660μm mediolaterally and fills intermediate and lateral portions of VII. The injection site from the first animal illustrated in Figure 2b fills the lateral and intermediate portions of the nucleus and measures 1,455μm rostrocaudally, 1,210μm dorsoventrally and 690μm mediolaterally. There is some spread into the perifacial zone and intermediate reticular region dorsally.

Figure 4 show a series of selected line drawings taken from coronal sections through Vo (injection in first animal) showing the location of ninety-one labeled Vo-VII projection neurons. The majority of labeled cells were in VL and DM and occupied the middle one-third of ipsilateral Vo. Labeled cells in VL outnumbered those in DM by a 2:1 ratio. A few labeled neurons were observed in BZ. Contralateral VL and DM also contained a few labeled cells. Injections in VII labeled VL and DM neurons characterized by spherical-shaped somata. These cell bodies could be characterized as medium-

sized (between 20μm and 30μm in diameter) with somatic cross-sectional areas of 100-550μm^2, and average cross-sectional areas of 289μm^2 (Figure 7,10). Although there were fewer neurons labeled in the caudal pole as compared to the middle of Vo, VL neurons continued to outnumber those in DM 2:1. BZ contained only one labeled cell which occupied its ventral half. Contralaterally, a few labeled neurons were located in VL. The cell bodies gave rise to bipolar dendritic fields (Figure 7,10). In the middle one-third of Vo, DM neurons were located ventromedially in the caudal most sections, whereas they became situated dorsolaterally as one moves rostrally (Figure 4). Labeled VL neurons were located more ventrally in caudal sections but filled the middle of the subdivison more rostrally. A few labeled neurons were found in the ventral and dorsal most regions of BZ. Contralaterally, there were a few labeled neurons in DM and VL. All of the Vo-VII projection neurons displayed basically bipolar-shaped dendritic fields (Figure 7,10).

At the rostral pole of Vo, DM and VL were sparcely filled with labeled neurons (Figure 4). No labeled neurons were found in BZ. Only one labeled cell was found contralaterally in VL.

NEURONS PROJECTING TO THE HYPOGLOSSAL NUCLEUS

Unilateral HRP deposits were localized within XII in two animals. The schematic drawing in Figure 2c illustrates two

injection sites while the photomicrograph in Figure 1c illustrates the injection site from the first animal. It measures 1,250μm rostrocaudally, 1,400μm dorsoventrally and 1,210μm mediolaterally as it fills the dorsoventral and rostrocaudal extent while filling approximately the medial three-fourths of the nucleus. The injection site in the second animal illustrated in Figure 2c fills the lateral half of the nucleus throughout its dorsoventral and rostrocaudal extent. The spread of HRP in this injection site measures 1,190μm rostrocaudally, 1,575μm dorsoventrally and 1,140 mediolaterally. There is some spread into the gigantocellular reticular region.

Figure 5 show a series of line drawings from coronal sections through Vo showing the location of labeled neurons as a result of the HRP injection described above. Fifty-nine neurons were labeled and distributed in nearly equal numbers in ipsilateral VL and DM in the middle one-third of Vo. In addition, a few labeled neurons were observed in ipsilateral BZ as well as contralateral DM. These labeled neurons in each of the subdivisions exhibited spherical-shape somata. (Figure 8,11) They could be identified as being small (< 25 μm in diameter) neurons with somatic cross-sectional areas of 100 to 450 μm^2 and average cross-sectional areas of 185μm^2 (Figure 8,11).

At the caudal pole of Vo, labeled neurons were sparse and widely scattered but appeared to be evenly distributed between

VL and DM (Figure 5). One labeled neuron was found in the ventral one-half of BZ. No neurons were located contralaterally. Small Vo-XII projection neurons, distributed equally throughout the nucleus, displayed both bipolar and multipolar-shaped dendritic fields (Figure 5).

The middle one-third of Vo, contained the majority of Vo-XII projection neurons. Distributed evenly between VL and DM, these labeled neurons were located in the medial portion of DM and throughout VL. A few labeled neurons were found contralaterally in DM with one labeled cell located in the ventral one-half of BZ.

The rostral pole of Vo was basically devoid of labeled neurons (Figure 5). Two labeled cells were found along the medial border of VL.

DISCUSSION

These anatomical studies show that Vo has predominantly ipsilateral efferent projections to Vmo, VII, and XII. Vo projection neurons are situated primarily in the middle third of the nucleus with the majority of them located in VL and DM subdivisions with only a few cells in BZ. Vo neurons innervating Vmo, VII and XII fall into three size ranges with small neurons projecting to Vmo and XII, medium size cells innervating VII and large-sized neurons forming terminal arbors in Vmo. These findings coupled with previous anatomical studies that show that DM, VL and BZ neurons receive morphologically and functionally distinct types of primary trigeminal afferents (6,7,8,9,10,11,12,45), suggest that Vo efferents to Vmo, VII, and XII provide multiple projections carrying different types of primary trigeminal afferent input to these cranial nerve motor nuclei. Projections to Vmo, VII, and XII from DM, VL and BZ most likely provide a route for Vonvolvement in complex reflexes (e.g., corneal reflex, orienting reflexes, jaw opening reflex) elicited by stimulation of different types of primary trigeminal afferents innervating the skin of the face, oral and nasal mucous membranes and muscles, tendons and bones of the jaw and face.

INJECTION SITES

Unilateral HRP injection sites in Vmo, VII and XII were

only considered effective if they filled a significant portion of the nucleus, with little spread into surrounding areas and if Vo contained densely filled neurons. The Vmo injection site in the first animal filled a significant amount of the nucleus without spread into surrounding areas. However, the number of labeled neurons in Vo was less than in the second animal which not only filled the nucleus but had some spread into adjacent intertrigeminal and peritrigeminal areas. Having fewer labeled cells in Vo after the injection in the first animal was probably due to the lack of HRP reaction product in the most dorsal and ventral extremes of the nucleus. It is important to note that the distribution of the labeled Vo cells was generally the same in both cases.

Injection sites in VII, in both animals, filled the dorsoventral and rostrocaudal extents of the nucleus, however, neither injections totally filled the medial aspect of the nucleus. These two cases showed similar distributions of labeled Vo neurons with fewer labeled cells present in the second animal. Injection sites which would include the most medial aspect of VII most likely would result in an increase in the number of labeled Vo cells but the distribution of labeled neurons would probably be similar.

For XII, the dorsoventral and rostrocaudal extent of the nucleus was filled by combining the data from the injection site in the second animal,which filled only the lateral one-half of the nucleus and the injection site in the first animal

which filled the medial two-thirds of the nucleus.

Vo PROJECTIONS TO Vmo

The organization of efferent projections from Vo to Vmo has been well established in previous anatomical studies (37,41,42,46) However, the specific morphological features of o-Vmo projection neurons, their locations in Vo subdivisions, as well as their distributions, have not been elucidated. A previous anatomical and electrophysiological study (41,42) demonstrated the existence of two distinct types f Vo projection neurons to cat Vmo. The first cell type displayed a cell body similar in size and shape to the large size Vo-Vmo projection neuron found in the present study. The second neuronal type was smaller than the first, and appeared to be morphologically similar to the small size Vo-Vmo projection neuron in this study. These findings substantiate those of the present study that two distinct types of Vo-Vmo projection neurons are present in Vo. The present study extends these findings by showing the two types of cells are found in DM and VL of rat Vo. The anatomical and electrophysiological study of Shigeniga, et al,(41,42) correlated size of Vo-Vmo projection neurons with low and high threshold mechanoreception and inhibitory and excitatory postsynaptic potentials suggesting that Vo-Vmo neurons play an important role as excitatory or inhibitory interneurons on masticatory motoneurons and may be involved in jaw reflexes related to jaw

movement or avoidance reactions. The large Vo-Vmo projection neurons received input from low-threshold mechanoreceptor afferents while the small Vo-Vmo projection neuron received nociceptive input from afferents innervating tooth pulp. The study of Shigeniga, et al (41,42) indicated that Vo-Vmo projection neurons form terminal arbors in the dorsolateral subdivision of Vmo and contain inhibitory or excitatory interneurons for jaw-closing motoneurons. The same study further suggested that due to differences in latencies, activation of large and small Vo-Vmo projection neurons may elicit fast and slow inhibitory postsynaptic potentials in masseter motoneurons which may cause inhibition of jaw reflexes in relation to the jaw movements or avoidance reactions.

An anterograde PHA-L study in the rat at the light microscopic level (44) showed that Vo-Vmo efferent axons displayed terminal axonal arbors of a single morphological type suggesting that small and large DM and VL neurons exhibit terminal arbors of similar morphology in Vmo. Based on these findings, further analyses including electron microscopy,evaluating the cytology and synaptic connections of Vo-Vmo efferents, are needed to ascertain whether or not Vo-Vmo projection neurons in different subdivisions of Vo have morphologically similar terminations in Vmo. It may be that these efferents differ in their synaptic vesicle size and shape; and synaptic junction morphology as well as in their

postsynaptic targets in Vmo.

Vo PROJECTIONS TO XII

A Vo-XII projection in the rat, shown in the present study, confirms those of the retrograde transport studies of Borke, et al, (2). In that study Borke, et al (2) described the Vo-XII projection as arising from neurons situated only in the dorsal portion of Vo where primary afferents from the mandibular division of the trigeminal nerve, innervating perioral and intraoral structures, terminate. Electrophysiological studies substantiate this view by showing a disynaptic pathway to XII from various branches of the mandibular nerve (33). The present study extends the findings of Borke, et al (2) by showing that approximately equal numbers of Vo-XII projection neurons are found dorsally in Vo (DM) as well as ventrolaterally (VL) in regions of Vo known to receive primary afferent input from maxillary and opthalmic divisions of the trigeminal nerve. Thus, it appears that, in the rat, Vo-XII projection neurons receive primary afferent input from the entire orofacial region. Both the present study and those of Borke, et al (2) agree that only one size of Vo neuron projects to XII.

Anterograde PHA-L studies (44) have reported two distinct types of Vo efferents arborizing in XII, while in the present study only one size of Vo-XII projection neuron was identified. The retrograde transport technique used in the

present study does not allow one to see the entire dendritic fields of labeled neurons. Therefore, it is possible that Vo-XII projection neurons with similar cell body size have quite different dendritic fields morphologically as well as morphologically different terminal axonal arborizations in XII. The fact that XII receives two types of Vo efferents suggests that at least two different types of orofacial sensory information are being transmitted to XII.

Mammalian XII receives afferent information from the nucleus of the tractus solitarius and the sensory trigeminal nuclei for reflex movements of the tongue in swallowing, chewing and sucking in response to gustatory and other stimuli from the oral and pharyngeal mucosae (1). Some of this trigeminal input undoubtedly is from Vo. Corticobulbar afferents send information directly to XII as well as indirectly through interneurons in the neighboring reticular formation. This input is processed to modulate motor output to the intrinisic and extrinsic muscles of the tongue (1).

Vo PROJECTIONS to VII

Mammalian VII has been described as having perioral and periorbital motoneurons in its intermediate subdivisions, innae and neck motoneurons in its medial subdivisions and proboscis motoneurons situated in its lateral subdivisions (64). The present study demonstrates the results of injections into lateral and intermediate VII subdivisions with slight

spread into medial subdivisions. The more lateral injection revealed the same distribution as the more intermediate-medial injection except that fewer total numbers of neurons were labeled. This finding suggests that the Vo-VII projection has a greater influence on pinnae and neck motoneurons in the rat than on perioral and periorbital motoneurons, although both inputs appear to be substantial.

Previous anterograde studies (44) have revealed that Vo projects to VII. Two morphologically distinct types of terminal axonal arborizations were found to be present in VII after a Vo injection. However, the present retrograde anatomical study suggests that there is one population of Vo-VII projection neurons based on cell body size. This situation could be the same as seen for Vo-XII projection neurons. That is, although there is one soma size, the cells may have structurally different dendritic fields and terminal axonal arborizations making the cells morphologically different from each other.

DUALITY OF Vo PROJECTIONS TO Vmo, VII AND XII.

The results of the present study suggest that some VL and DM neurons may project to more than one cranial nerve motor nucleus. Vo-XII projection neurons and several Vo-Vmo projection neurons had similar sized cell bodies as well as number of cells projecting to these nuclei. Based on these findings its possible that one small DM or VL neuron projects

to both Vmo and XII. The anterograde studies of Smith and Falls (64) also contribute to this theory as one type morphological type of terminal axonal arbor was found in XII and VII after a Vo injection, which suggests that one Vo neuron could also be projecting to both VII and XII.

FUNCTIONAL CONSIDERATIONS

The circuitry described above suggests that Vo plays an important role in not only reflexes dealing with Vmo, VII and XII but also in fine tuning oral motor function, i.e. mastication, deglutition, vocalization, and facial expression. As mechanoreceptive and nociceptive information from the facial skin, oral and nasal cavities, and teeth are received in Vo, it is important for this information to be sent to VII. For example, a Vo-VII route projection for the corneal reflex is important to protect the eye, as well as causing changes in facial expression secondary to pain or touch. This latter function is evident in humans with oral or facial pain where facial expression is affected significantly. A Vo-VII projection also must underlie chewing or sucking responses to placing food in the mouth. A Vo-XII projection must underlie the masticator reflex as well as mastication,deglutition and vocalization. A Vo-Vmo projection may be essential for reflex modulation such as in the jaw-opening reflex in which the contractions of the masseter, temporalis, and medial pterygoid muscles are inhibited as a result of painful pressure applied

to the teeth. As information is collected and processed in Vo, it can have a significant influence on the gross and fine motor control of the oral facial region.

Figure 1a,b,c: Horseradish peroxidase (HRP) Injection Sites

Representative transverse sections (a-c) of HRP injection sites (IS) in trigeminal motor nucleus (VMO), facial nucleus(VII), and hypoglossal nucleus (XII). The injection sites are, for the most part, confined to their respective nuclear areas.

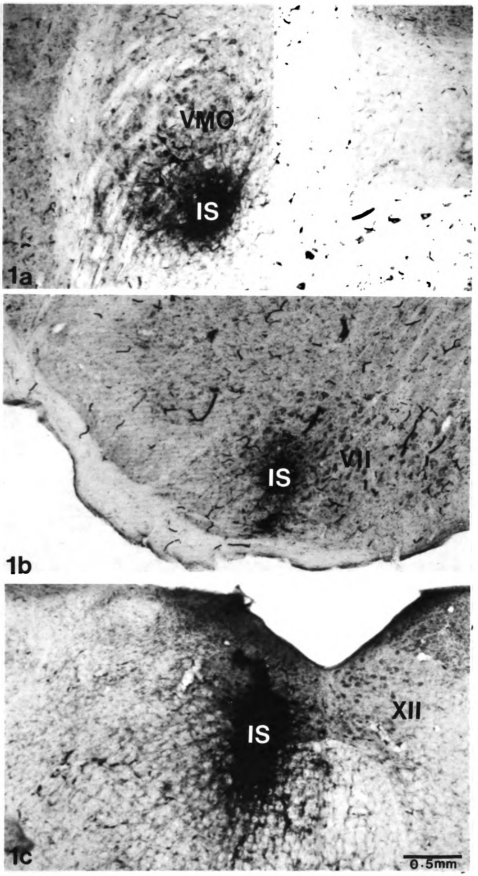

Figure 1

Figure 2a,b,c: Schematic Drawings of HRP Injection Sites

Schematic drawings of representative transverse sections (a-c) showing two HRP injection sites (IS) each in Vmo, VII, and XII. The injection sites were, for the most part, confined to their respective nuclear areas. Vp, principal sensory nucleus; sol, solitary nucleus; svt, sensory trigeminal tract; Vi, nucleus interpolaris; Vo,nucleus oralis.

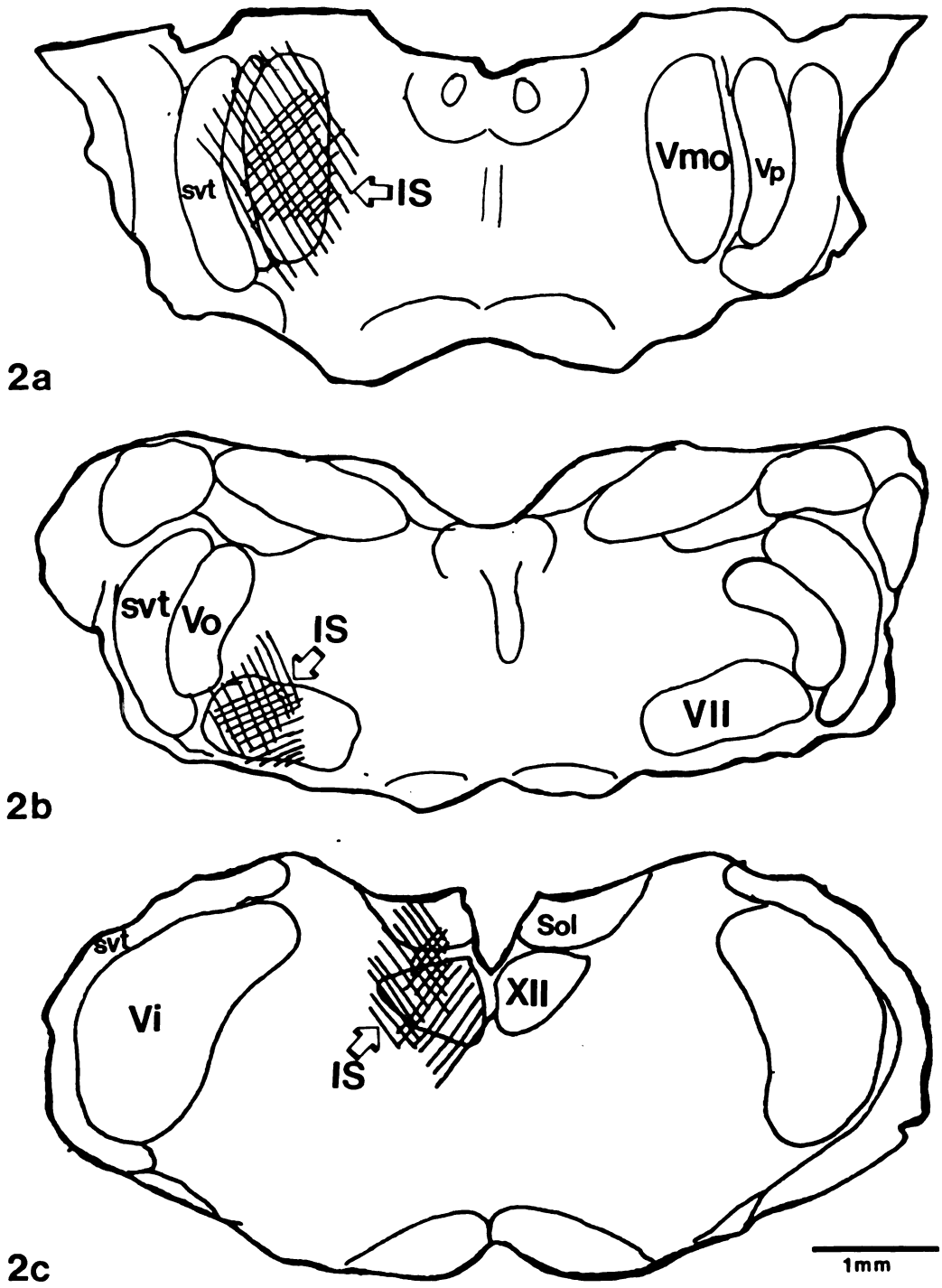

Figure 2

Figure 3: Distribution of Vo-Vmo Projection Neurons

Schematic drawings of representative transverse sections through the entire rostrocaudal length of Vo demonstrating the distribution of Vo-Vmo Projection Neurons. Drawings are from caudal to rostral including all the DM subdivisions: caudal dorsomedial subdivision (CDM); Middle dorsomedial subdivision dorsal zone (MDMd) and ventral zone (MDMv); and rostral dorsomedial subdivision (RDM). Vo-Vmo Projection neurons are distributed primarily throughout ipsilateral Vo, with the majority located in the MDMv and MDMd as well as VL. BZ, border zone subdivision; svt, spinal trigeminal nucleus.

Figure 4: Distribution of Vo-VII Projection Neurons

Schematic drawings of representative transverse sections through the entire rostrocaudal length of Vo demonstrating the distribution of Vo-VII Projection Neurons. Vo-VII projection neurons are distributed primarily throughout ipsilateral Vo with the majority located in the MDMv and MDMd as well as VL.

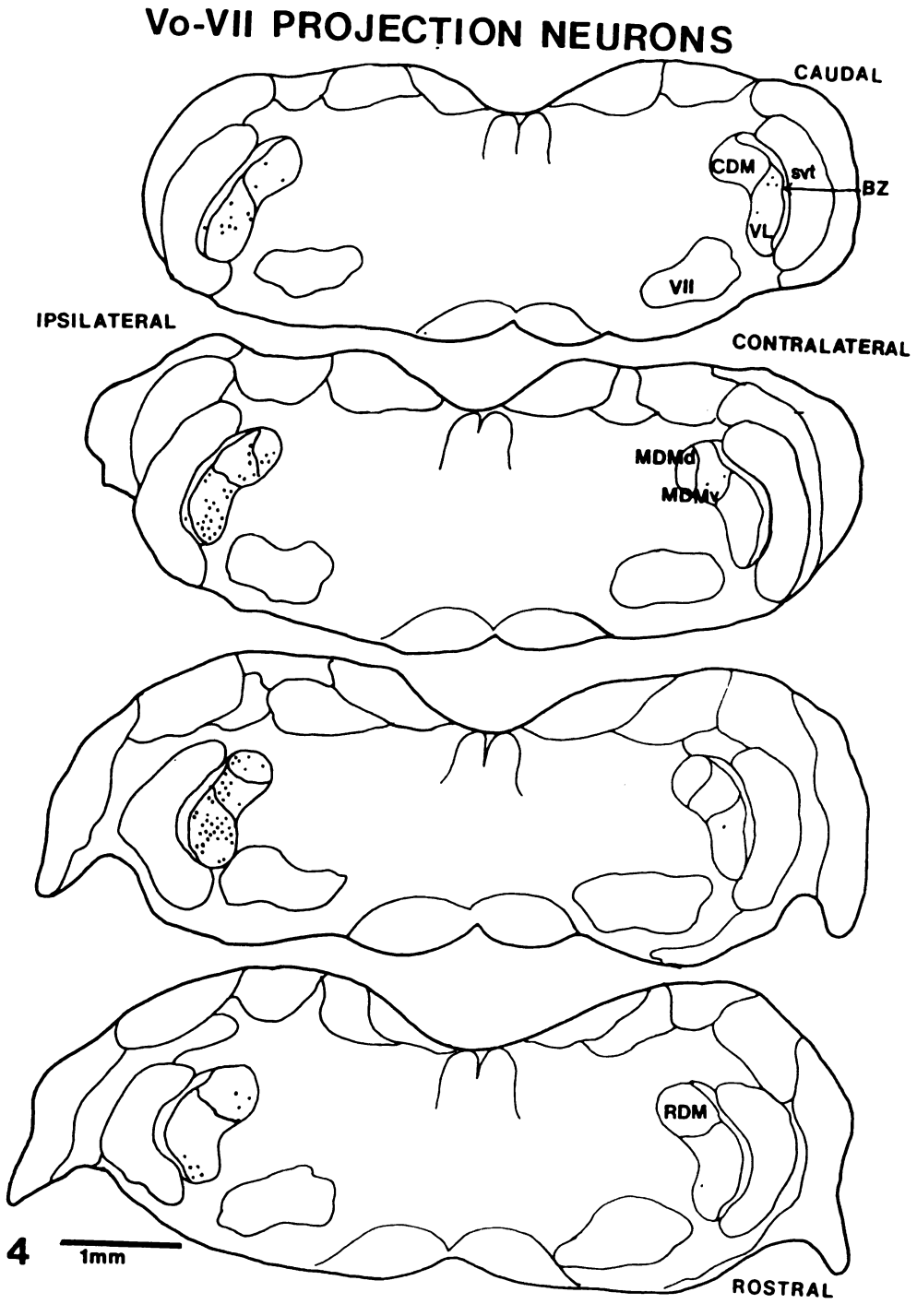
Vo-VII PROJECTION NEURONS
CAUDAL
CDM
svt
BZ
VL
VII
IPSILATERAL
CONTRALATERAL
MDMd
MDMv
RDM
4
1mm
ROSTRAL

Figure 4

Figure 5: Distribution of Vo-XII Projection Neurons

Schematic drawings of representative transverse sections through the entire rostrocaudal length of Vo demonstrating the distribution of Vo-XII Projection Neurons. Vo-XII projection neurons are distributed primarily throughout ipsilateral Vo with the majority of located in MDMv and MDMd as well as VL.

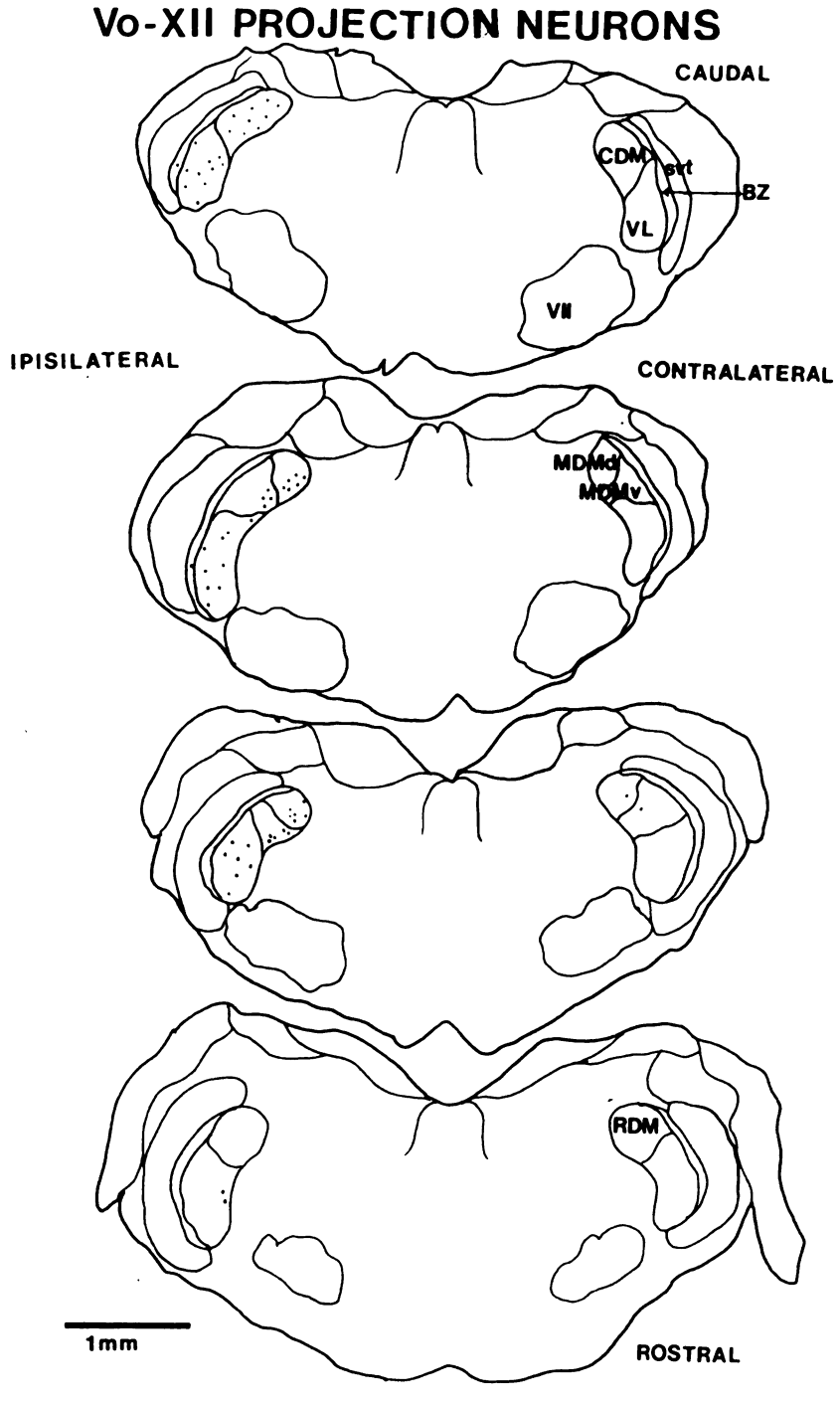
Vo-XII PROJECTION NEURONS
CAUDAL
CDM
str
BZ
VL
VII
IPISILATERAL
CONTRALATERAL
MDMd
MDMv
RDM
1mm
ROSTRAL

5

Figure 5

Figure 6: Diagrams of Vo-Vmo Projection Neurons

Schematic drawings of representative neurons in VL and DM projecting to Vmo. Two morphologically distinct types of large and small neurons were identified projecting to Vmo.

Figure 7: Diagrams of Vo-VII Projection Neurons

Schematic drawings of representative neurons in VL and DM projecting to VII. One distinct type of medium sized projection neuron was identified projecting to VII.

Figure 8: Diagrams of Vo-XII Projection Neurons

Schematic drawings of representative neurons in DM and VL projecting to XII. One distinct type of small projection neuron was identified projecting to XII.

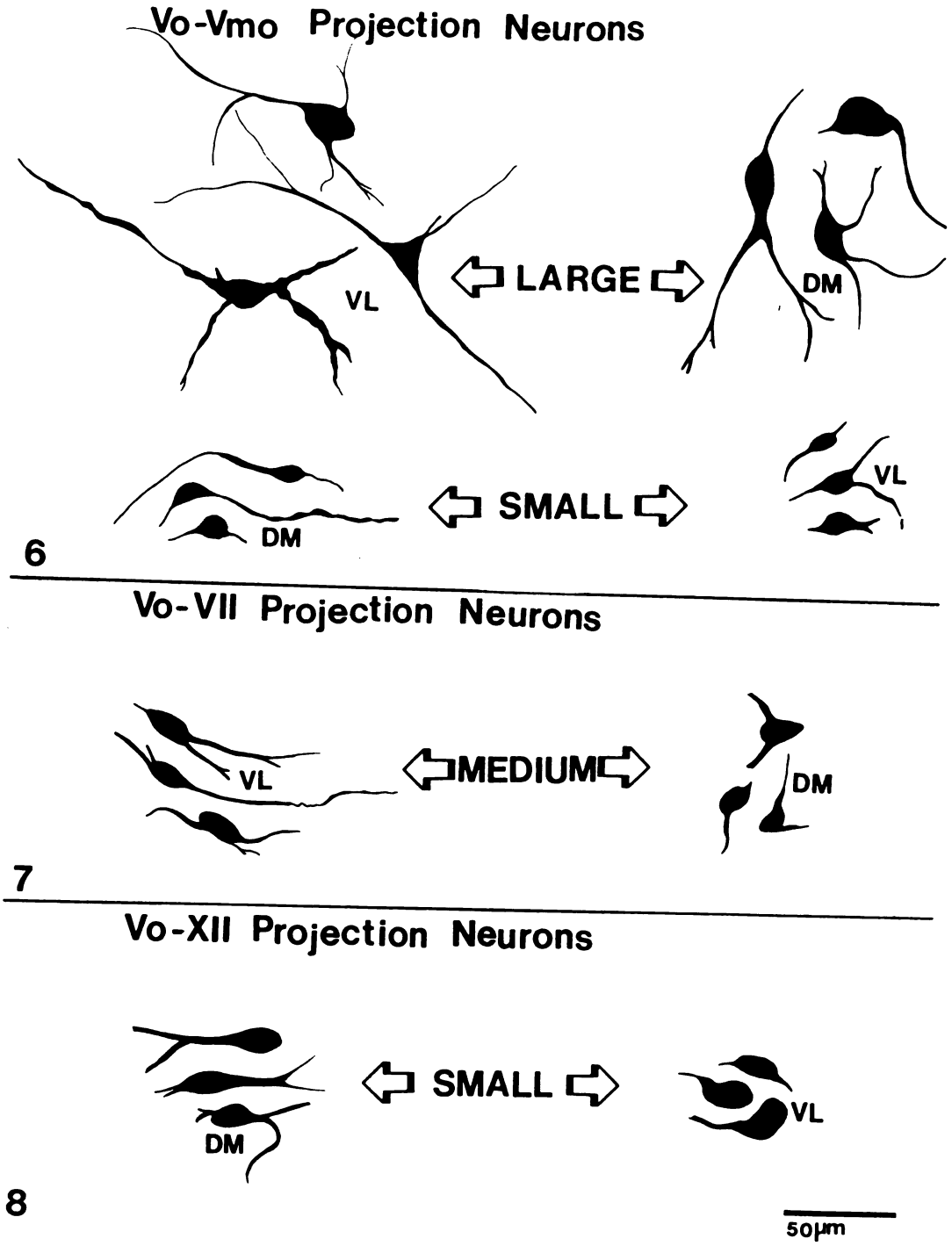
Vo-Vmo Projection Neurons
VL
LARGE
DM
DM
SMALL
VL
6
Vo-VII Projection Neurons
VL
MEDIUM
DM
7
Vo-XII Projection Neurons
DM
SMALL
VL
8
50µm

Figures 6,7,8

Figure 9a,b,c,d,e,f: Photomicrographs of Vo-Vmo Projection Neurons

Photomicrographs were taken of representative HRP-filled Vo-Vmo projection neurons. Two morphologically distinct Vo-Vmo projection neurons (Fig 7) were identified. In 9a and b are small neurons while in 9 c-f large cells size are shown. Cells of both sizes are found in DM (a,c,d) and VL (b,e,f).

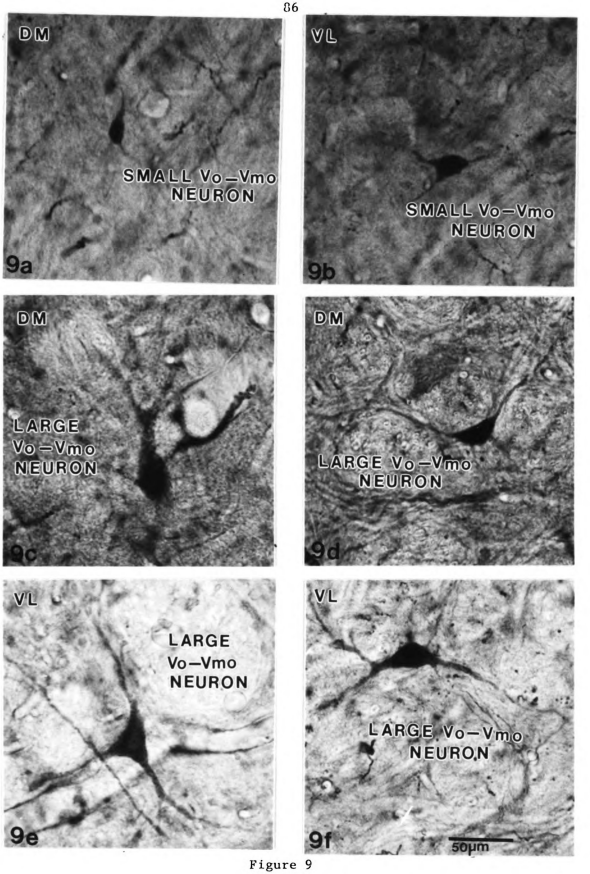
DM
SMALL Vo–Vmo NEURON
9a
VL
SMALL Vo–Vmo NEURON
9b
DM
LARGE Vo–Vmo NEURON
9c
DM
LARGE Vo–Vmo NEURON
9d
VL
LARGE Vo–Vmo NEURON
9e
VL
LARGE Vo–Vmo NEURON
9f
50µm

Figure 9

Figure 10 a,b: Photomicrographs of Vo-VII Projection Neurons

Photomicrographs of medium-sized HRP-filled Vo-VII projection neurons in DM (a) and VL (b) of Vo.

Figure 11 a,b: Photomicrographs of Vo-XII Projection Neurons

Photomicrographs of the one distinct small sized Vo-XII projection neuron in DM (a) and VL (b).

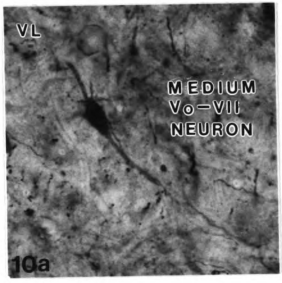

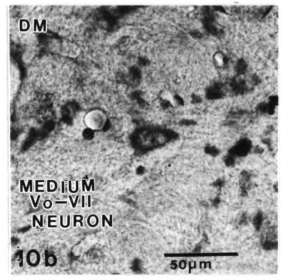

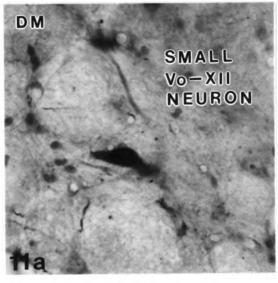

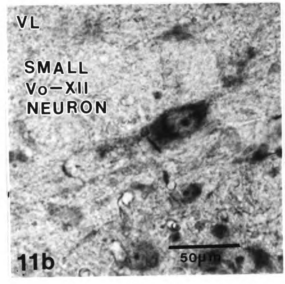

Figures 10, 11

Figure 12: Somatic Cross-Sectional Areas of Vo-Vmo, Vo-VII and Vo-XII Projection Neurons

The percentage of cells identified in all of the cases involved in this study are graphically displayed to show their somatic cross-sectional area. The graph displays all three motor nuclei where neurons from Vo are projecting with the number of neurons per each nucleus shown in the box.

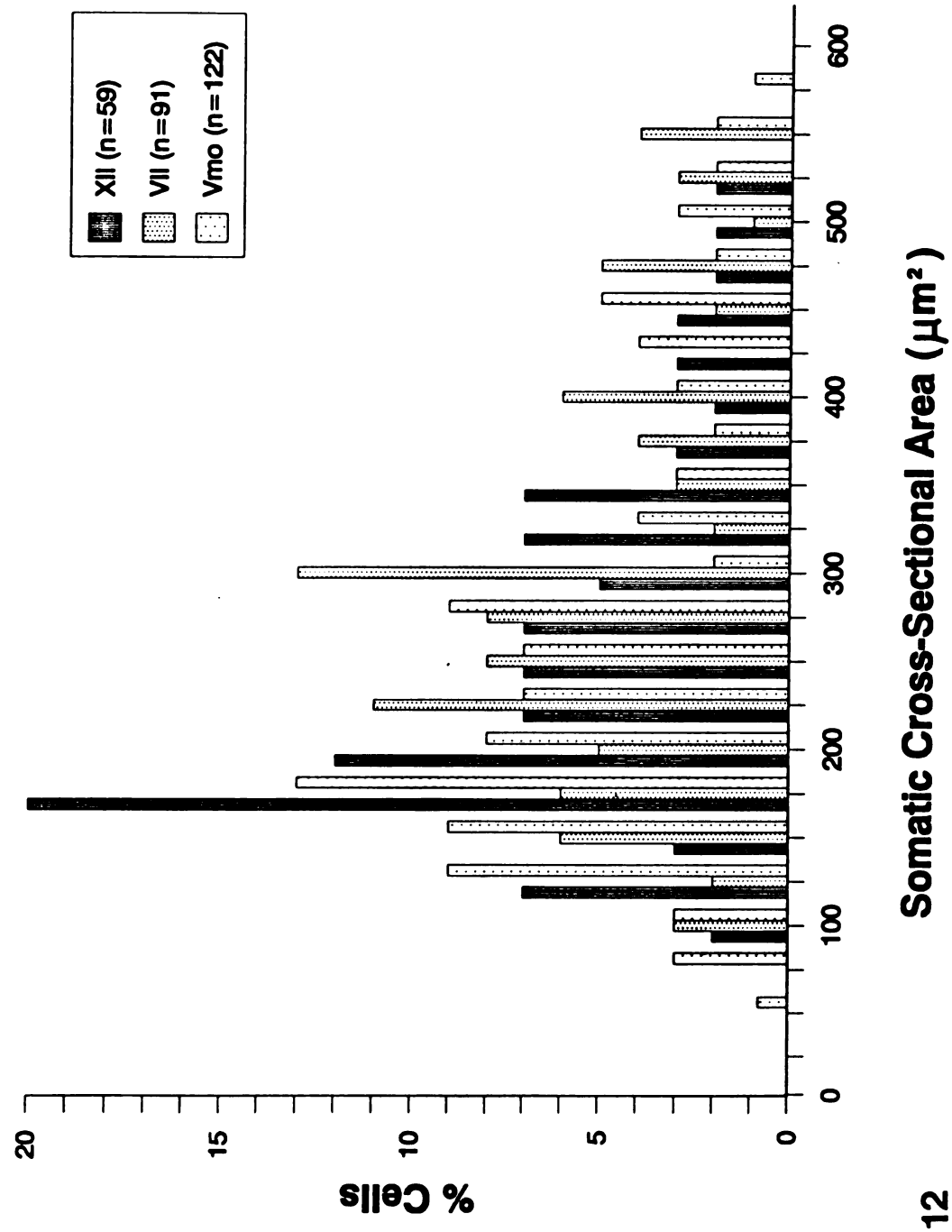
XII (n=59)
VII (n=91)
Vmo (n=122)
% Cells
0
5
10
15
20
0
100
200
300
400
500
600
Somatic Cross-Sectional Area (μm²)
12

Figure 12

Figure 13: Somatic Cross-Sectional Area of Vo-Vmo, Vo-VII, and Vo-XII Projection Neurons in DM

Graph showing the percentage of DM cells with their cross-sectional areas at 25μm intervals projecting to each motor nucleus.

Figure 14: Somatic Cross-Sectional Area of Vo-Vmo, Vo-VII, Vo-XII Projection Neurons in VL

Graph showing the percentage of VL cells with their cross-sectional areas at 25μm intervals projecting to each motor nucleus.

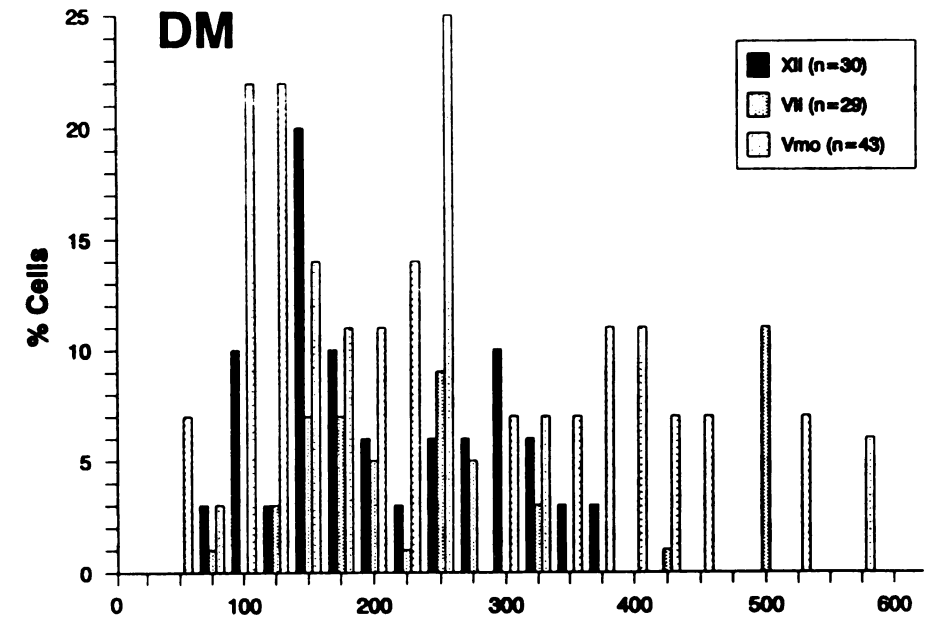

13

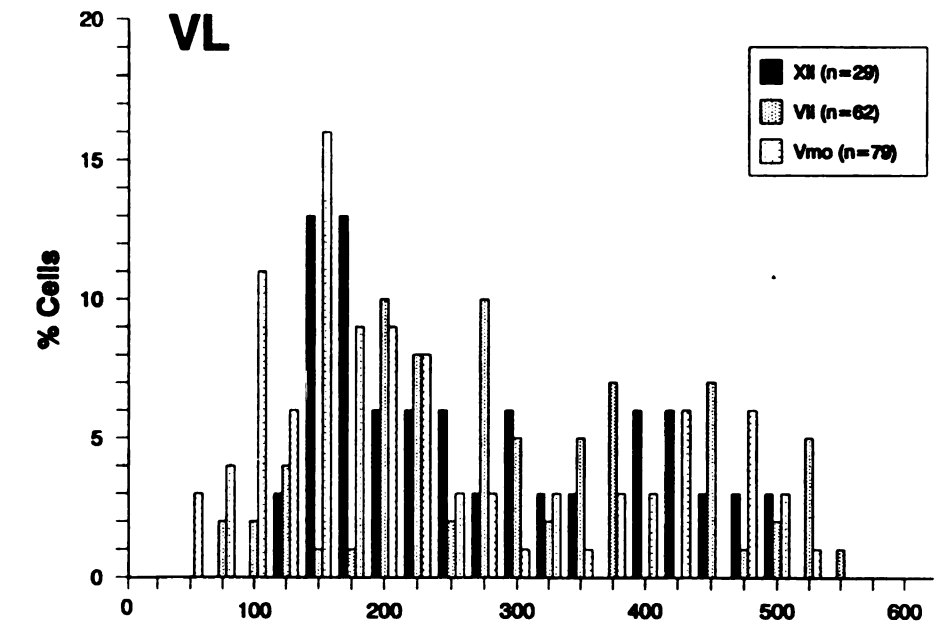

14

Figures 13,14

BIBLIOGRAPHY

1. Barr, M.L., and Kiernan, J.A. (1988) The Human Nervous System 5th Edition. Pennsylvania.

2. Borke, R. C., and M. E. Nau and R. L. Ringler., Jr.(1983) Brain Stem Afferents of Hypoglossal Neurons in the Rat. Brain Research. 269:47-55.

3. Bruce, L. L., J. G. Mchaffie and B. E. Stein (1987) The organization of trigeminotectal and trigeminothalamic neurons in rodents: A double-labeling study with fluorescent dyes. J. Comp. Neurol. 262:315-530.

4. Erzurumlu, R. S., and H. P. Killackey (1979) Efferent connections of the brainstem trigeminal complex with the facial nucleus of the rat. J. Comp. Neurol. 188:75-86.

5. Erzurumlu, R. S., C. A. Bates, and H. P. Killackey (1980) Differential organization of thalamic projection cells in the brain stem trigeminal complex of the rat. Brain Res. 198:427-433.

6. Falls, W. M. (1983a) A Golgi type II neuron in trigeminal nucleus oralis: A Golgi study in the rat. Neurosci. Letts. 41:11-7.

7. Falls, W. M. (1983b) Light and EM analysis of identified trigeminospinal projection neurons in rat trigeminal nucleus oralis. Anat. Rec. 205:55A.

8. Falls, W. M. (1984a) Termination in trigeminal nucleus oralis of ascending intratrigeminal axons originating from neurons in the medullary dorsal horn: An HRP study employing light and electron microscopy. Brain Res. 29:136-140.

9. Falls, W. M. (1984b) Axonal endings terminating on dendrite of identified large trigeminospinal projection neurons in rat trigeminal nucleus oralis. Brain Res. 324:335-341.

10. Falls, W. M. (1984c) The morphology of neurons in trigeminal nucleus oralis projecting to the medullary dorsal horn (trigeminal nucleus caudalis): A retrograde HRP and golgi study. Neurosci. 13:1279-1298.

11. Falls, W. M. (1986a) Morphology and synaptic connections of unmyelinated primary axons in the border zone of rat trigeminal nucleus oralis. Neurosci. Letts. 70:342-347.

12. Falls, W. M. (1986b) Morphology and synaptic connections of myelinated primary axons in the ventrolateral portion of rat trigeminal nucleus oralis. J. Comp. Neurol. 244:96-110.

13. Falls, W. M. (1987) Direct connections of primary trigeminal afferent axons with trigeminocerebellar projection neurons in the border zone of rat trigeminal nucleus oralis. Neurosci. Letts. 83:247-252.

14. Falls, W. M. and M. M. Alban. (1986a) Morphological features of identified trigeminocerebellar projection neurons in the border zone of rat trigeminal nucleus oralis. Somatosensory Res. 4:1-12.

15. Falls, W. M. and M. M. Alban. (1986b) Morphology and synaptic connections of small myelinated primary trigeminal axons arborizing among neurons in the border zone of rat trigeminal nucleus oralis. Somatosensory Res. 4:97-110.

16. Falls, W.M., B.J. Moore, and M.T. Schneider. (1990) Fine structural characteristics and synaptic connections of trigeminocerebellar projection neurons in rat trigeminal nucleus oralis. Somatosensory and Motor Res. 7:1-18.

17. Falls, W. M., R. E. Rice and J. P. Van Wagner. (1985) The dorsomedial portion of trigeminal nucleus oralis (Vo) in the rat: Cytology and projections to the cerebellum. Somatosensory Res. 3:89-118.

18. Fukushima, T., and F. W. L. Kerr (1979) Organization of trigeminothalamic tracts and other thalamic afferent systems of the brainstem in rat: presence of gelatinosa neurons with thalamic connections. J. Comp. Neurol. 183:169-184.

19. Hayashi, H. (1982) Differential terminal distribution of single large cutaneous afferent fibers in the spinal trigeminal nucleus and in the cervical spinal dorsal horn. Brain Res., 244:173-177.

20. Hayashi, H. 1985. Morphology of terminations of small and large myelinated trigeminal primary afferent fibers in the cat. J. Comp. Neurol. 240:71-89.

21. Hayashi, H., R. Sumino and B. J. Sessle (1984) Functional organization of trigeminal subnucleus interpolaris: Nociceptive and innocuous afferent inputs, projections to thalamus, cerebellum, and spinal cord, and descending modulation from periaqueductal gray. J. Neurophysiol. 51:890-905.

22. Hockfield, S. and S. Gobel (1978) Neurons in and near nucleus caudalis with long ascending projection axons demonstrated by retrograde labeling with horseradish peroxidase. Brain Res. 204:415-420.

23. Huerta, M. F. A. Frankfurter, and J. K. Harding (1983) Studies of the principal sensory and spinal trigeminal nuclei of the rat: projections to the superior colliculus, inferior olive and cerebellum. J. Comp. Neurol. 220:147-167.

24. Kaiga, Y., (1980) Linguo-hypoglossal reflex elicited by mechanical stimulation in rabbits. J. Osaka Odont. Soc., 43:449-460.

25. Leong, S. K., J. Y. Shieh and W. C. Wong (1984) Localizing spinal-cord-projecting neurons in adult albino rats. J. Comp. Neurol. 228:1-17.

26. Liu, D. and Y. Hu (1988) The central projections of the great auricular nerve primary afferent fibers -- an HRP transganglionic tracing method. Brain Res. 445: 205-210.

27. Marfurt, C. F. and D. F. Turner (1984) The central projections of tooth pulp afferent neurons in the rat as determined by the transganglionic transport of horseradish peroxidase. J. Comp. Neurol. 223:535-547.

28. Mizuno, J., Yasui, Y. Nomura, S., Itoh, K., Konishi, A., Takada, M. and Kudo, M. (1987) A light and electron microscopic study of premotor neurons for the trigeminal motor nucleus. J. Comp. Neurol., 215:184-198.

29. NIH Guide for the Care and Use of Laboratory Animals. NIH, 9000 Rockville Pike, Bethesda, MD. 20892, 1985.

30. Paxinos, G. and C. Watson (1986) The Rat Brain Sterotaxic Coordinates 2d Edition. New York.

31. Ruggiero, D. A., C. A. Ross and D. J. Reis (1981) Projections from the spinal trigeminal nucleus to the entire length of the spinal cord in the rat. Brain Res. 23265:225-233.

32. Shigenaga, Y., T. Okamoto, T. Nishimori, S. Suemune, I.D. Nasution, I.C. Chen, K. Tsuru, A. Yoshida, K. Tabuchi, M. Hosoi, and H. Tsuru. (1986a). Oral and Facial Representation in the trigeminal Principal and Rostral Spinal Nuclei of the Cat. J. Comp. Neurol. 244;1-18.

33. Shigenaga, Y., S. Suemune, M. Nishimura, T. Nishimori, H. Sato, H. Ishidori, A. Yoshida, K. Tsuru, Y. Tsuiki, Y. Dateoka, I.D. Nasution, and M. Hosoi. (1986b). Topographic representation of lower and upper teeth within the trigeminal sensory nuclei of adult cat as demonstrated by the transganglionic transport of horseradish peroxidase. J. Comp. Neurol. 251:299-316.

34. Silverman, J. D., and L. Kruger (1985) Projections of the rat trigeminal sensory nuclear complex demonstrated by multiple fluorescent dye retrograde transport. Brain Res. 361:383-388.

35. Smith, L.A. and Falls, W.M. (1994) Topographical distribution and morphological features of second order projections from identified subdivisional areas of rat trigeminal nucleus oralis. Ph.D. Thesis. Dept. of Anatomy, Michigan State University, East Lansing, MI.

36. Sohn, D. J. and Falls, W.M. (1994) Morphology, Cytology and synaptic relations of primary trigeminal axons terminating in the dorsomedial subdivision of rat trigeminal nucleus oralis. Ph.D. Thesis. Dept. of Anatomy. Michigan State University, East Lansing, MI.

37. Travers, J. and R. Norgren, (1983) Afferent projections to the oral motor nuclei in the rat. J. Comp. Neurol., 220:280-298.